1 **Multiple knockout mutants reveal a high redundancy of phytotoxic compounds that**
2 **determine necrotrophic pathogenesis of *Botrytis cinerea***

3

4 **Thomas Leisen[1], Janina Werner[1,2], Patrick Pattar[1], Edita Ymeri[1], Frederik Sommer[3],**
5 **Michael Schroda[3], David Scheuring[1], Matthias Hahn[1,*]**

6 [1]Department of Biology, Phytopathology group, Technische Universität Kaiserslautern, Paul-
7 Ehrlich Straße 22, D-67663 Kaiserslautern, Germany
8 [2] Present address: Botanical Institute and Cluster of Excellence on Plant Sciences (CEPLAS),
9 BioCenter, University of Cologne, Zülpicher Str. 47a, Cologne, 50674, Germany
10 [3]Department of Biology, Molecular Biotechnology & Systems Biology group, Technische
11 Universität Kaiserslautern, Paul-Ehrlich Straße 22, D-67663 Kaiserslautern, Germany

12

13 *Author for correspondence, e-mail: hahn@biologie.uni-kl.de

14

15

16 **Abstract**

17 *Botrytis cinerea* is a major pathogen of more than 1400 plant species. During infection, the
18 kills host cells during infection and spreads through necrotic tissue, which is believed to be
19 supported by induction of programmed plant cell death. To comprehensively evaluate the
20 contributions of most of the currently known plant cell death inducing proteins (CDIPs) and
21 metabolites for necrotrophic infection, an optimized CRISPR/Cas protocol was established
22 which allowed serial marker-free mutagenesis to generate Botrytis mutants lacking up to 12
23 different CDIPs. Infection analysis revealed a decrease in virulence with increasing numbers
24 of knockouts, and differences in the effects of knockouts on different host plants. The *on
25 planta* secretomes obtained from these mutants revealed substantial remaining necrotic
26 activity after infiltration into leaves. Our study has addressed for the first time the functional
27 redundancy of virulence factors of a fungal pathogen, and demonstrates that *B. cinerea*
28 releases a highly redundant cocktail of proteins and metabolites to achieve necrotrophic
29 infection of a wide variety of host plants.

30

31

32 **Introduction**

33 *Botrytis cinerea* is considered as one of the most important plant pathogenic fungi, causing
34 severe pre- and postharvest losses on fruits, vegetables and other crops worldwide (Elad Y
35 *et al.* 2016). The fungus attacks its host plants preferentially under humid and cool
36 conditions. Before and after invasion into the plant tissue, the hyphae kill the surrounding
37 host cells and spread through the dying tissue, followed by the development of a superficial
38 mycelium which has the typical grey mold appearance and releases a plethora of conidia into
39 the air. Mechanisms that have been proposed to promote necrotrophic infection of *B.
40 cinerea* are the secretion of plant cell death inducing proteins (CDIPs) and cell wall degrading

41 enzymes, the release of phytotoxic metabolites and organic acids, and the acidification of
42 the host tissue (Müller *et al.* 2018; Veloso and van Kan, 2018; Zhu *et al.* 2017). Furthermore,
43 the fungus can suppress host defense gene expression by the release of small interfering
44 RNAs (Weiberg *et al.* 2013), and it is able to detoxify plant defence compounds such as
45 camalexin and tomatine via efflux transporters or by enzymatic modification (Stefanato *et*
46 *al.* 2009; You and van Kan, 2021).

47 How host cell death is induced is not fully understood, but there is evidence that
48 necrotrophic fungi actively trigger the hypersensitive response (HR), a plant-specific type of
49 programmed cell death linked to strong defence reactions including an oxidative burst
50 (Govrin and Levine, 2000; Veloso and van Kan, 2018). Several secreted compounds have
51 been described as virulence factors. *B. cinerea* releases two major phytotoxic metabolites,
52 the sesquiterpenoid botrydial and the polyketide botcinin, which have been shown to be
53 together required for full virulence (Dalmais *et al.* 2011; Pinedo *et al.* 2008). Plant cell wall
54 degrading enzymes (CWDE) are required for tissue mazeration by necrotrophic pathogens,
55 but because of their redundancy, the contributions of individual members are difficult to
56 determine. *B. cinerea* mutants lacking either of the two major endopolygalacturonases, PG1
57 and PG2, showed impaired lesion formation (Have *et al.* 1998; Kars *et al.* 2005). An endo-
58 arabinanase (BcAra1) was found to be required for full infection of Arabidopsis but
59 dispensable for infection of tobacco (Nafisi *et al.* 2014). Further, a cellobiohydrolase and a
60 β-endoglucanase were reported to contribute to plant infection (Li *et al.* 2020). Several
61 CWDEs of *B. cinerea* are CDIPs, inducing necrosis of different plant tissues. Necrotic activity
62 was found to be independent of enzymatic activity for two xylanases, Xyn11A and Xyl1, and
63 the xyloglucanase XYG1. For Xyn11A and Xyl1, peptides of 25 and 26 amino acids,
64 respectively, were identified that induced cell death (Frías *et al.* 2019; Yang *et al.* 2018), and
65 for XYG1 two exposed loops of the folded protein were identified as being essential to induce
66 cell death (Zhu *et al.* 2017). Mutants lacking Xyn11A and Xyl1 showed impaired infection
67 (Noda *et al.* 2010; Yang *et al.* 2018). *B. cinerea* also secretes CDIPs without known enzymatic
68 activity. Nep1 and Nep2, which belong to a large family of plant necrosis and ethylene
69 inducing proteins in fungi, oomycetes and bacteria, induce pores in membranes of
70 dicotyledonous plants (Seidl and van den Ackerveken, 2019). *B. cinerea* mutants lacking
71 either Nep1 or Nep2 showed normal virulence (Cuesta Arenas *et al.* 2010). The cerato-
72 platanin Spl1, was found to be required for full infection, whereas elimination of IEB1 had no
73 effect on virulence (Frías *et al.* 2011; Frías *et al.* 2016). The recently identified CDIP Hip1 was
74 found to require its tertiary structure for phytotoxic activity. While knockout mutants
75 showed normal infection, strains overexpressing Hip1 showed revealed slightly increased
76 virulence compared to the wild type (WT) strains (Frías *et al.* 2016; Jeblick *et al.* 2020).

77 Similar to infection by *B. cinerea*, treatment of leaf tissues with individual CDIPs usually
78 results in HR-like programmed cell death (Frías *et al.* 2011; Frías *et al.* 2013; Frías *et al.* 2016;
79 Yang *et al.* 2018; Zhu *et al.* 2017). CDIPs oft act as pathogen associated molecular patterns
80 (PAMPs) that are recognized by pattern recognition receptors (PRRs) in the plant membrane,
81 leading to the so-called PAMP-triggered immunity (PTI) (Thomma *et al.* 2011). A PAMP-like
82 behavior of CDIPs was indicated by the observation that their activity was dependent on the
83 presence of the PRR coreceptors BAK1 and/or SOBIR1 in the treated plants (Franco-Orozco
84 *et al.* 2017; Frías *et al.* 2011; Yang *et al.* 2018; Zhu *et al.* 2017), and PRRs for Nep1/Nep2,

85   Xyn11A and PG1/PG2 have already been identified (Albert *et al.* 2015; Ron and Avni, 2004;
86   Zhang *et al.* 2014). Recently, a novel *B. cinerea* CDIP was discovered that is translocated into
87   plant cells, but it does not seem to contribute to infection (Bi *et al.* 2021).

88   Based on the data summarized above, it is evident that *B. cinerea* secretes a mixture of
89   phytotoxic compounds to kill host cells, and triggering of HR seems to play an essential role
90   in this process. Because elimination of single CDIPs or phytotoxins has been shown to have
91   either no or only limited effects on pathogenesis, a comprehensive approach is required for
92   understanding how and to what extent CDIPs contribute to necrotrophic pathogenesis. The
93   goal of this study was to create single and multiple mutants of genes for most of the currently
94   known CDIPs and phytotoxic metabolites, in the same genetic background and one
95   laboratory, and to evaluate their contribution to the infection process of *B. cinerea*. By
96   applying an improved version of a recently developed CRISPR/Cas9-based method for
97   marker-free genome editing (Leisen *et al*. 2020), we generated multiple mutants lacking up
98   to 12 CDIPs and phytotoxins. These mutants were unaffected in their growth and
99   differentiation *in vitro*, but showed significantly impaired virulence compared to WT on
100 different host tissues. These data highlight the role and the complexity of the toxic
101 secretome for necrotrophic infection of *B. cinerea*.
102

103 **Results**

104 <u>Generation of *B. cinerea* single and multiple CDIP mutants</u>

105 Before the CRISPR/Cas protocol for marker-free mutagenesis was available (Leisen *et al*.
106 2020), different selection markers were used to generate single and up to quadruple mutants
107 by standard mutagenesis, using knockout constructs integrated into the target genes by
108 homologous recombination. In addition to the established markers conferring resistance to
109 hygromycin (HygR), nourseothricin (NatR) and fenhexamid (FenR), the anilinopyrimidine
110 fungicide cyprodinil (Cyp)(Heye *et al.* 1994) was developed as a new marker for selection in
111 *B. cinerea*. The mode of Cyp resistance (CypR) has been uncovered by a functional genomics
112 approach (Mosbach *et al.* 2017). Many CypR *B. cinerea* field strains contain a mutation
113 leading to an L412F exchange of a mitochondrial NADPH kinase encoded by *Bcpos5*. A CypR
114 selection marker was generated by integrating *Bcpos5^{L412F}* into a constitutive expression
115 cassette (Fig. 1A). Functionality of the CypR marker was confirmed by targeted mutagenesis
116 of several genes, which yielded robust numbers of transformants, with a low fraction of
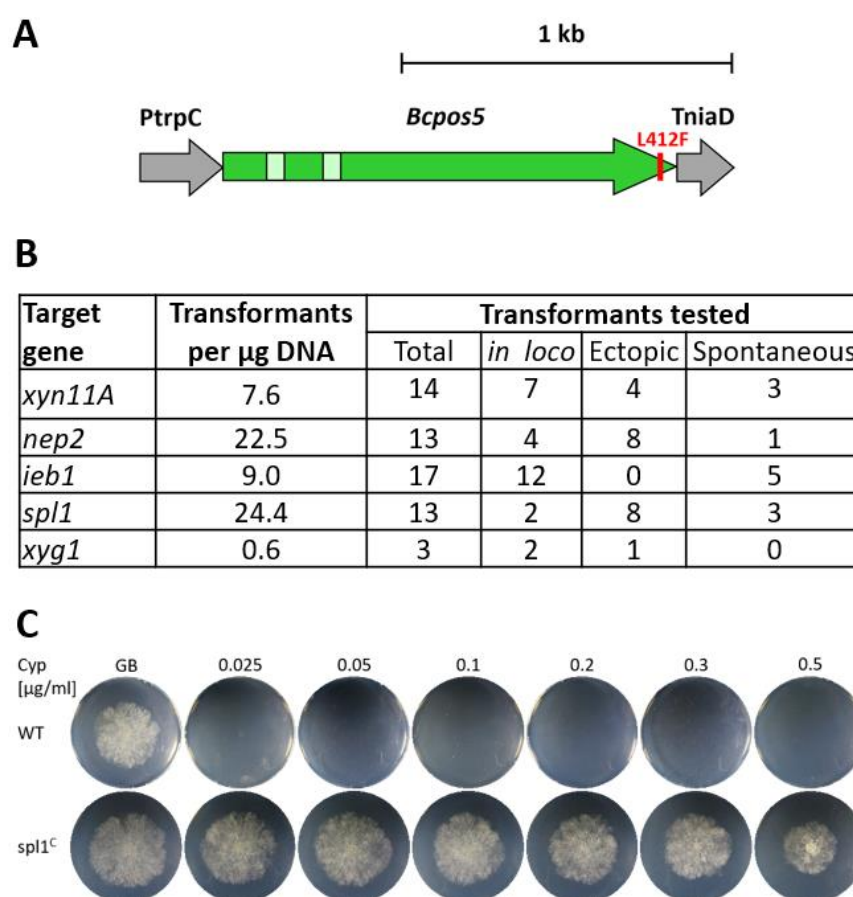117 spontaneous CypR mutants (Fig. 1B,C).

118

3

A

B

Target gene	Transformants per µg DNA	Transformants tested			
		Total	*in loco*	Ectopic	Spontaneous
xyn11A	7.6	14	7	4	3
nep2	22.5	13	4	8	1
ieb1	9.0	17	12	0	5
spl1	24.4	13	2	8	3
xyg1	0.6	3	2	1	0

C

Figure 1: Establishment of cyprodinil resistance (CypR) as a novel selection marker for *B. cinerea*. A: CypR cassette containing a 344 bp promoter fragment of *Aspergillus nidulans trpC*, and a 146 bp terminator fragment of *B. cinerea niaD*. B: Transformation efficiency with the CypR cassette and characterization of the CypR transformants. *in loco*: Correct knockout mutants (replacement of WT DNA by CypR cassette). Ectopic: Detection of CypR cassette outside of target gene. Spontaneous: FenR 'transformants' lacking the CypR cassette. C: Growth of a CypR resistant transformant (spl^C), and the sensitive *B. cinerea* WT strain on agar plates with GB5 minimal medium containing different Cyp concentrations.

The genes analysed by mutagenesis include most of the currently known *B. cinerea* CDIPs and phytotoxins (Table 1). Single knockout mutants were generated for the previously characterized genes *xyn11A*, *spl1*, *xyg1*, *ieb1*, and *nep2*. Furthermore, we constructed mutants of *gs1* encoding a putative glucoamylase previously reported as a CDIP (Zhang *et al.* 2015), and of *plp1* (PAMP like protein) encoding the homolog of a CDIP of the apple pathogen *Valsa mali* named VmE02 (Nie *et al.* 2019). All mutants showed normal vegetative growth and differentiation *in vitro*. When infection experiments were performed with tomato and *Phaseolus* bean leaves and apple fruits, no significant differences in virulence compared to WT were observed (Fig. S1). These results demonstrated that none of the deleted genes alone play a major role for infection on any of the tested plants. These results are inconsistent with previous studies, which reported reduced virulence of *B. cinerea xyn11A*, spl1 *and xyl1* mutants (Brito *et al.* 2006; Frías *et al.* 2011; Noda *et al.* 2010). Next, a quadruple mutant (4x^R: *xyn11A spl1 nep1 nep2*) was generated by using four different resistance markers, including the newly established CypR marker. As shown below, the 4x^R mutant was

4

143 weakly impaired in virulence, besides a minor growth retardation. This would be consistent
144 with weak phenotypes of the single mutants that are too small to be detected in our infection
145 assays.

146

147

148 Table 1: Cell death-inducing (CDI) metabolites and CDIPs of *Botrytis cinerea*

	k.o. effects	*in planta* expression[1]	PRR	Evidence for PRR coreceptors	References
CDI metabolites					
Botrydial	yes[2]	++	no	---	Dalmais *et al.* 2011
Botcinic acid		++	no	---	
CDIPs (non-enzymatic)					
Nep1	no	+/+++	RLP23	BAK1, SOBIR1	Cuesta Arenas *et al.* 2010; Albert *et*
Nep2	no	++	RLP23	BAK1, SOBIR1	*al.* 2015; Ono *et al.* 2020
Spl1 (cerato-platanin)	yes	+++	yes[§]	BAK1	Frías *et al.* 2011
IEB1	no	+++	yes[§]	no	González *et al.* 2017
Hip1	no	+++	yes[§]	no	Jeblick *et al.* 2020
PIP1	no	+	RE02	BAK1, SOBIR1	Nie *et al.* 2019, 2021
CDIPs: Enzymes[3]					
Xylanase Xyn11A	yes	++/+++	LeEIX2	no	Noda *et al.* 2010; Ron and Avni, 2004
Xyloglucanase Xyg1	no	++	yes	BAK1, SOBIR1	Zhu *et al.* 2017
Xylanase Xyl1	yes	+	yes	BAK1, SOBIR1	Yang *et al.* 2018
Glucoamylase Gs1	n.a.	++	yes	no	Zhang *et al.* 2015
Polygalacturonase PG1	yes	+++	RBPG1	BAK1, SOBIR1	Have *et al.* 1998; Kars *et al.* 2005; Zhang
Polygalacturonase PG2	yes	+++	RBPG1	BAK1, SOBIR1	*et al.* 2014

149 [1] Based on reads per kilobase million values from RNA sequencing data from infected tomato
150 leaves (Müller *et al.* 2018); Jan van Kan, unpublished); +++: RPKM >1000; ++: RPKM 100-1000; +:
151 RPKM <100.
152 [2] No effects of single k.o., reduced virulence of double k.o.
153 [3] CDI activity independent of enzyme activity (except for PG1, PG2)

154

155

Development of a CRISPR/Cas method for rapid generation of homokaryotic, multiple knockout mutants

158 We have recently described a powerful CRISPR/Cas-based method for *B. cinerea* gene editing
159 without introducing resistance markers into the transformants. It is based on
160 cotransformation of Cas9-sgRNA RNPs with an unstable telomere vector into protoplasts,
161 which allows transient selection of transformants containing the desired editing events
162 (Leisen *et al.* 2020). For improved serial mutagenesis, the protocol was modified to generate
163 deletions by two RNPs targeting one gene, without addition of a repair template, which
164 results in excision of the sequence between the cleavage sites by non-homologous end
165 joining (NHEJ). When the protocol was tested for knockout of *spl1*, several thousand FenR
166 transformants were obtained, and 68% of them verified by PCR analysis as being edited with
167 the correct deletion. For serial mutagenesis, two genes were targeted simultaneously by
168 using four RNPs in each transformation. These experiments usually yielded high editing rates,
169 resulting in the isolation of mutants containing the expected single and double deletions

170   (Table 2). Unexpectedly, a large fraction of the primary transformants appeared to be
171   homokaryotic, and complete loss of the deleted DNA in these transformants was confirmed
172   after a single spore isolation step. This represents a great advancement over traditional
173   transformation methods for *B. cinerea*, which usually resulted in heterokaryotic
174   transformants that had to be purified by several rounds of single spore isolation before
175   homokaryosis was achieved (Hahn and Scalliet, 2021).

178   Table 2: Serial deletion of *B. cinerea* genes encoding CDIPs and phytotoxic metabolites.

Transf. Round	Strain (mutant) used for transformation		Genes targeted for k.o.	Characterization of transformants						
	Name	Genotype		Total	Tested	Deletion 1*	Homo-karyons	Deletion 2*	Homo-karyons	Δ1 + Δ2*
1	WT	WT	*spl1*	>1000	22	15 (68%)	6	n.a.	n.a.	n.a.
2	spl1&	*spl1*	*nep1, nep2*	157	26	6 (23%)	4	7 (27%)	5	2 (8%)
3	3x&	*spl1 nep1 nep2*	*xyn11A, ieb1*	>1000	104	13 (13%)	10	6 (6%)	4	0 (0%)
4	4x&	*spl1 nep1 nep2 xyn11A*	*hip1, xyg1*	>5000	70	57 (81%)	50	54 (77%)	49	40 (57%)
5	6x	*spl1 nep1 nep2 xyn11A hip1 xyg1*	*plp1, ieb1*	>1000	46	20 (43%)	17	10 (22%)	8	4 (9%)
6	8x	*spl1 nep1 nep2 xyn11A hip1 xyg1 plp1 ieb1*	*xyl1, gs1*	>1000	64	31 (48%)	n.a.	8 (13%)	n.a.	8 (13%)
7a	10x	*spl1 nep1 nep2 xyn11A hip1 xyg1 plp1 ieb1 xyl1 gs1*	*pg1, pg2*	102	56	5 (9%)	5	1 (2%)	1	1 (2%)
7b			*bot2, boa6*	>1000	105	3 (3%)	2	26 (25%)	n.a.	3 (3%)

	Name	Genotype of mutants derived from strain 10x transformed with *pg1, pg2* (11x, 12xpg) or *bot2, boa6* (12xbb)
	11x	*spl1 nep1 nep2 xyn11A hip1 xyg1 plp1 ieb1 xyl1 gs1 pg1*
	12xpg	*spl1 nep1 nep2 xyn11A hip1 xyg1 plp1 ieb1 xyl1 gs1 pg1 pg2*
	12xbb	*spl1 nep1 nep2 xyn11A hip1 xyg1 plp1 ieb1 xyl1 gs1 bot2 boa6*

179   *Number and percentage of transformants with confirmed deletions in gene 1 (Δ1), gene 2 (Δ2), or both genes.
180   & Mutants were not phenotypically characterized.

182   The improved transformation protocol was used for serial inactivation of up to 12 genes
183   encoding CDIPs and key enzymes for biosynthesis of the phytotoxins, botrydial and botcinin.
184   The expected gene deletions, and the absence of remaining WT DNA in the deleted regions
185   were verified by PCR (Fig. S2). Sequencing revealed in most cases precise (±2 bp) excisions
186   as predicted from the RNP-directed DNA cleavage sites, except for the Δ12xpg mutant in
187   which a 3 kb larger deletion than expected had occurred in *pg2* (Table S1).

189   <u>Phenotypic analysis of multiple mutants lacking up to 12 CDIPs and phytotoxins</u>

190   All mutants displayed growth and sporulation similar to WT (Fig. 2A, B). Sclerotia formation,
191   which is induced by cultivation in complete darkness, was also unaffected (Fig. 2C). When

192 incubated on glass surfaces for two days, WT germlings form large aggregates of appressoria-
193 like structures, so-called infection cushions. They are believed to represent alternative
194 infection structures to simple appressoria (Choquer *et al.* 2021). Infection cushions with
195 similar morphology were formed by the WT and the 12xpg and 12xbb mutants (Fig. 2D).
196 When inoculated onto killed onion epidermal layers, conidia WT and mutants showed a
197 similar infection behaviour, by forming short germ tubes following by penetration into host
198 cells and formation of thick intracellular hyphae (Fig. 2E). These data confirmed that none of
199 the secreted proteins are involved in vegetative growth, reproduction and pathogenic
200 differentiation on artificial surfaces and killed host tissue.
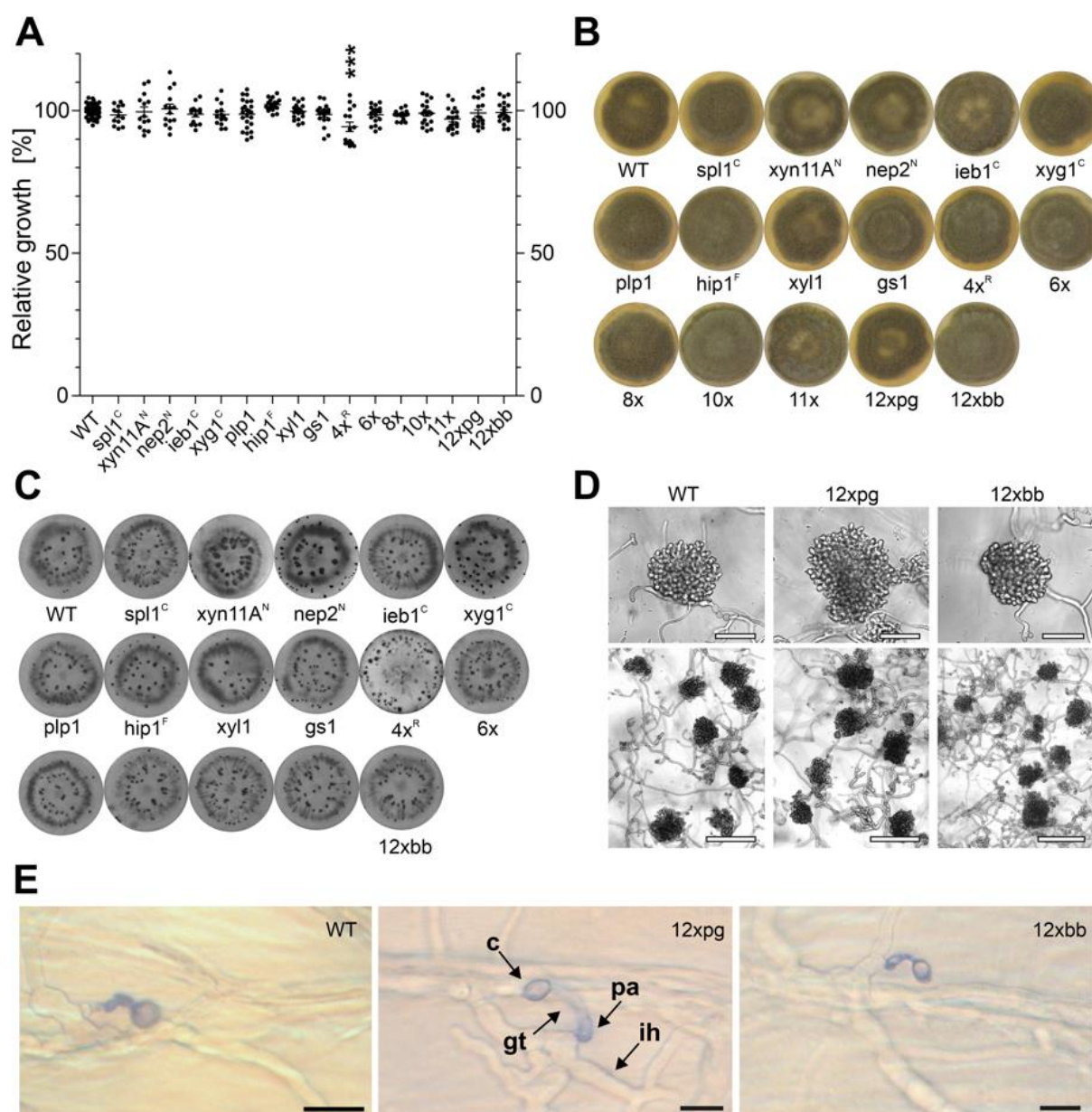
201

202

204 Figure 2: Growth and differentiation of *B. cinerea* B05.10 (WT) and mutants generated in this study. A: Relative
205 radial growth on GB5 minimal agar medium with 25 mM glucose (3 days). The p values by one way ANOVA
206 followed by Dunnett's multiple comparisons post-hoc test are indicated; ***: $p < 0.001$. B: ME plates incubated
207 for 10 days under permanent light to induce conidia formation. C: ME plates incubated for 14 days in darkness

208 to induce sclerotia formation. Mutants marked with superscript letters were generated with resistance
209 markers. D: Infection cushions formed on glass slides after 48 h. Upper scale bars: 50 µm; lower scale bars: 150
210 µm. E: Penetration of onion epidermis cells by germinated conidia of WT, 12xpg and 12xbb mutants. Superfical
211 structures (conidium, germ tube and appressorium) are stained with trypan blue, whereas intracellular hyphae
212 remain unstained. Scale bars: 10 µm.

213

214 To test the effects of multiple knockouts on infection, leaves of *Phaseolus* bean, tomato and
215 maize, and apple fruits were inoculated, and necrosis formation quantified after 48 to 96 h
216 (Fig. 3). On all tested tissues, infection efficiency of the mutants decreased with increasing
217 number of deleted genes. On bean leaves and apple fruit, the mutants revealed a stronger
218 reduction in virulence than on tomato and maize leaves. For example, the 10x mutant
219 formed lesions which were only ca. 60% in size of WT lesions on bean leaves and apple, but
220 similar or only slightly smaller lesions on tomato and maize leaves. Compared to the 10x
221 mutant, 11x, 12xpg and 12xbb mutants showed further reductions of lesion sizes, except on
222 maize leaves. These comparisons allowed to assign contributions to virulence for *pg1* (10x
223 vs. 11x), *pg1* plus *pg2* (10x vs. 12xpg), encoding endopolygalacturonases, and *bot2* plus *boa6*
224 encoding key biosynthesis enzymes for botrydial and botcinin (Fig. 3). The effects of *pg1* and
225 *pg2* were confirmed by the reduced virulence of a *pg1 pg2* double mutant mutant, generated
226 by classical mutagenesis with selection markers, on all tested tissues (Fig. S3), in accordance
227 to previous results (Have *et al.* 1998; Kars *et al.* 2005). The effects of *bot2* and *boa6*
228 knockouts were most evident by the low virulence of the 12xbb mutant on apple. This was
229 confirmed by the infection phenotype of a previously generated *bot2 boa6* double mutant
230 (Leisen *et al.* 2020), which showed considerable reduction in lesion formation on apples
231 (Fig. S4). These results are consistent with published data (Dalmais *et al.*, 2011). Despite their
232 reduced virulence, the 12xpg and 12xbb mutants were eventually able to sporulate on
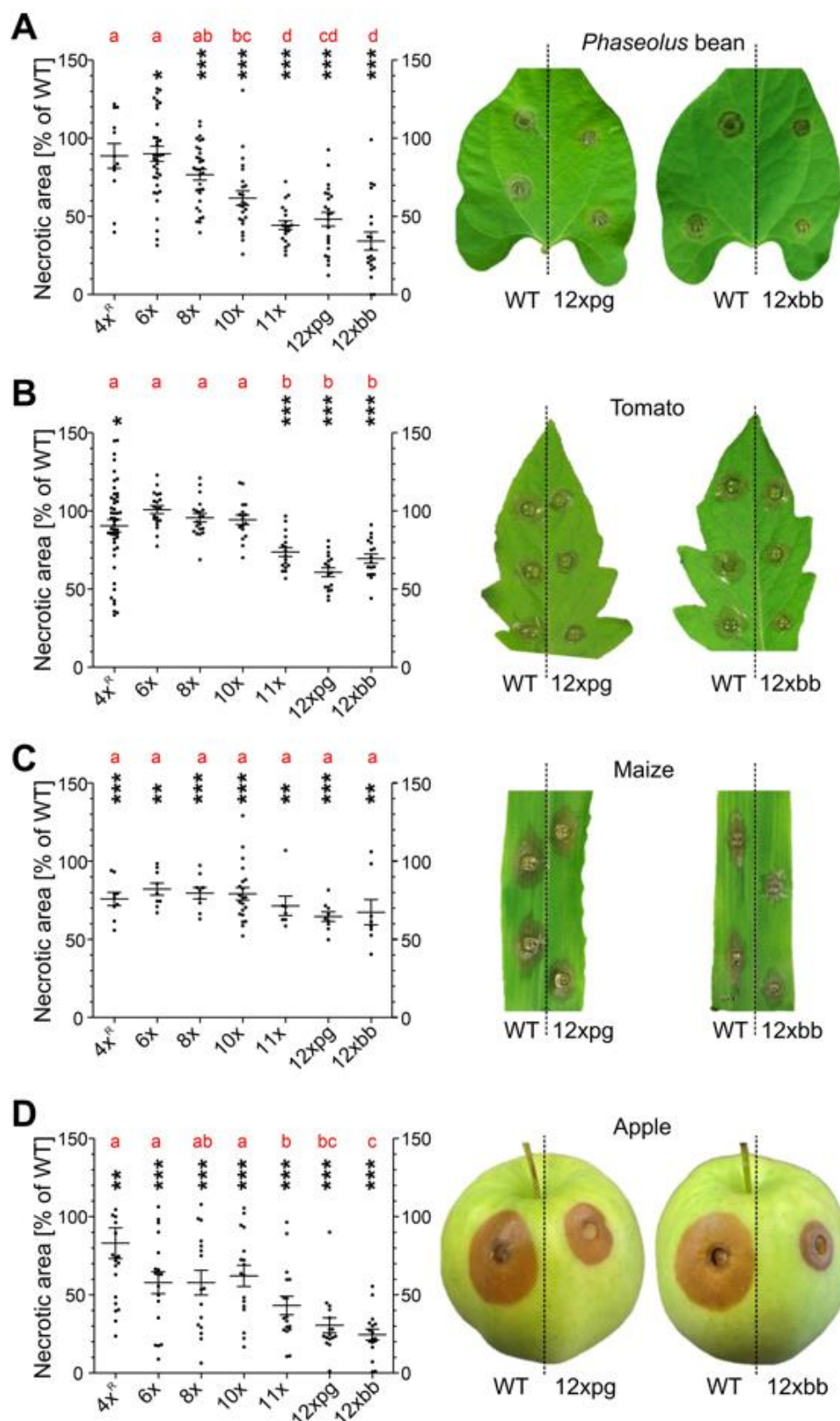233 infected bean and tomato leaves, similar to WT (Fig. S5).

Figure 3: Infection tests of multiple CDIP/ phytotoxin mutants. A: Attached *Phaseolus* bean leaves (48 h). B: Detached tomato leaves (48 h). C: Detached maize leaves (72 h). D: Apple fruits (96 h). The p values by one-sample t test to a hypothetical value of 100% (WT) are indicated. * p value < 0.05; ** p value < 0.01; *** p value < 0.001. Results of Tukey's multiple comparison test are displayed with compact letter display. The pictures show lesions caused by 12xbb and 12xpg mutants in comparison to WT.

9

Microscopic analysis of infection of WT and multiple mutants

The infection process of *B. cinerea* can be divided into penetration, primary lesion formation, lesion expansion and sporulation. To investigate whether the reduced virulence of the 12x mutants was related to defects in early stages of differentiation and infection, microscopic studies were performed. On *Phaseolus* leaves, host cell killing by both mutants was substantially reduced after 24 h (Fig. 4). These data show that the CDIPs deleted in these mutants are involved in the early stages of lesion formation on unwounded leaf tissue.
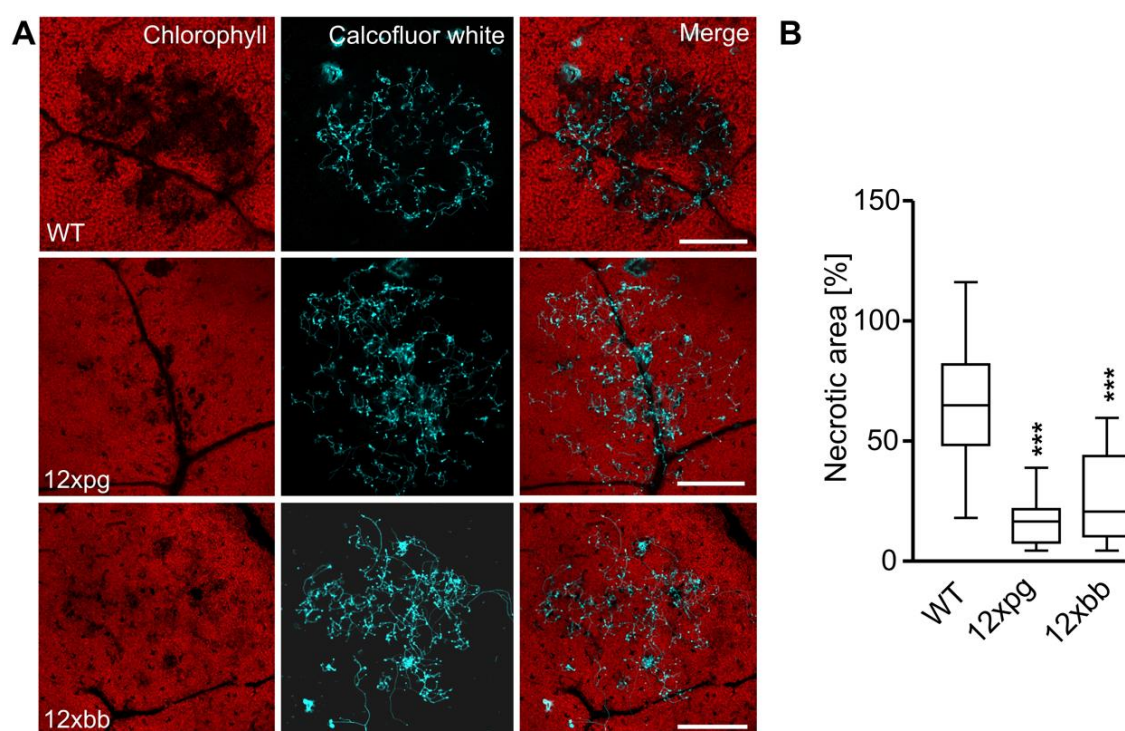

Figure 4: Microscopic analysis of early stage of infection of *B. cinerea* WT and mutants. Fungal hyphae were stained with calcofluor white, host cell death is visible by loss of autofluorescence. A: Host cell killing on *Phaseolus* leaves (24 h). Scale bars: 500 μm. B: Quantification of host necrosis. One-way ANOVA followed by Dunnett´s multiple comparison post hoc test ***$p < 0.001$.

Analysis of the secretomes of WT and multiple mutants

To verify the loss of proteins encoded by the deleted genes in the mutants, an proteomic analysis of *on planta* produced secretomes was performed according to (Müller *et al.* 2018). Out of the 12 CDIPs analysed, nine could be detected in the WT secretome, consistent with previous studies (Zhu *et al.* 2017; Müller *et al.* 2018). In all mutants, proteins were missing when the respective gene had been deleted (Table S2). Since most of the deleted CDIPs are highly expressed in the WT, we checked whether their loss was compensated by overexpression of other proteins in the secretomes of the 10x, 11x, 12xpg and 12xbb mutants. However, analysis of the proteome data using the Perseus bioinformatic platform (Tyanova and Cox, 2018) did not reveal evidences for differential protein abundance in the WT and mutant secretomes.

The *on planta* secretomes of *B. cinerea* are highly phytotoxic when infiltrated into leaves (Jeblick *et al.* 2020; Zhu *et al.* 2017). Similar toxicity was observed for the secretomes of WT

266 and up to 8x mutants. The secretomes of 10x, 12xpg and 12xbb mutants showed reduced
267 cell death inducing activity. Compared to 10x, the secretomes of 12xpg and 12xbb showed
268 decreased activity on *V. faba* and *N. benthamiana*, respectively, indicating differential
269 effects of the loss of PG1/PG2 (in 12xpg) and botrydial/botcinin (in 12xbb) on the different
270 plant species (Fig. 5A-D). As the 10x and the 12xbb mutant differed in their ability to
271 synthesize botrydial and botcinin, we investigated the contribution of the two phytotoxins.
272 Secretomes collected from the two mutants were fractionated by ultrafiltration through a
273 membrane with 10 kDa molecular weight cut off. No protein could be detected in the
274 filtrates, and only the filtrate of the 10x but not the 12x mutant caused necrosis, which could
275 be attributed the presence and absence of botrydial and botcinin, respectively (Fig. 5E).
276 Heating of the 10x mutant filtrate to 95°C for 20 min did not signficantly reduce its phytotoxic
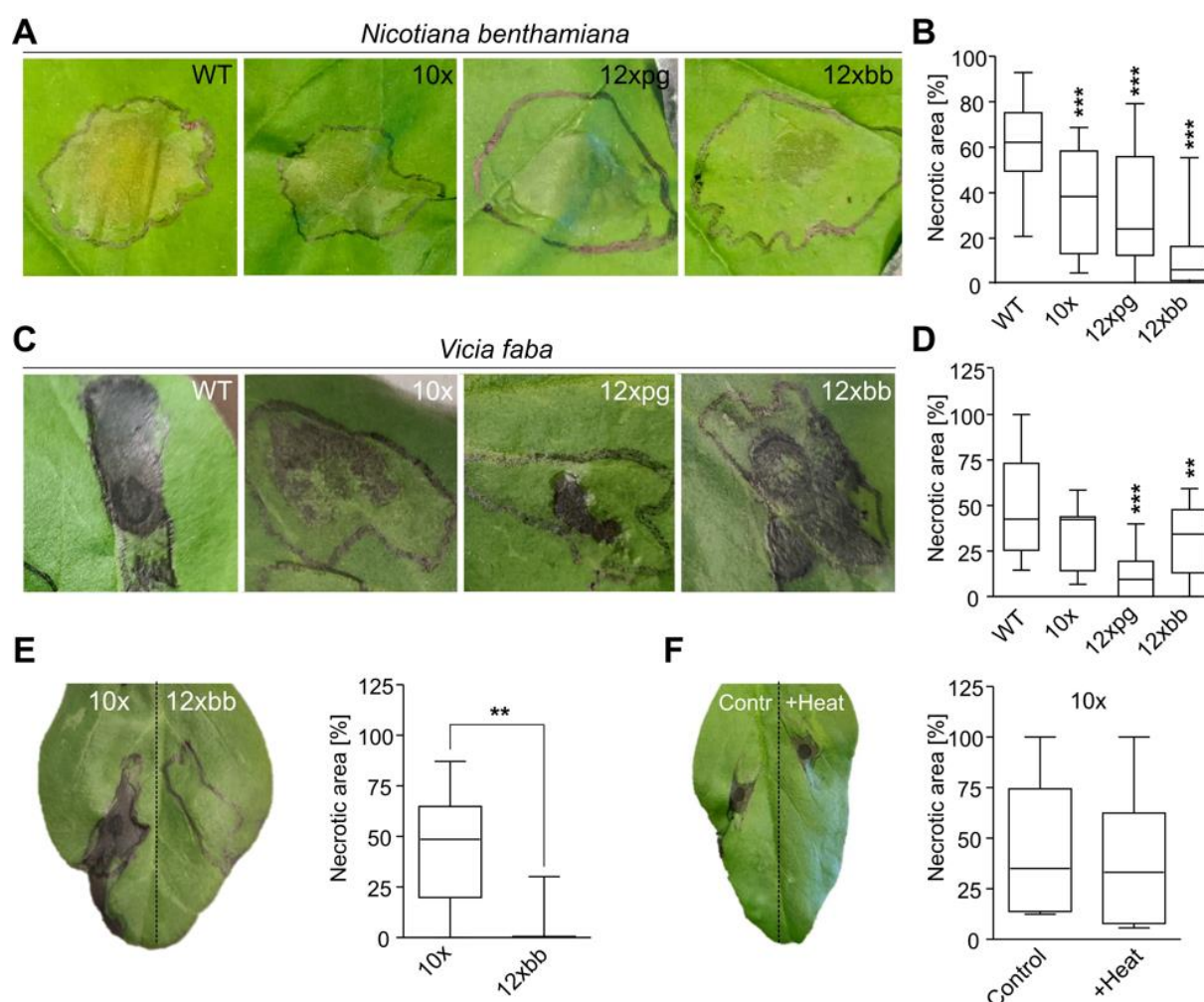277 activity (Fig. 5F).

281 Figure 5: Cell death inducing activity of *B. cinerea on planta* secretomes. A-D: Necrotic lesions caused by WT
282 and mutant secretomes (2 µg ml^{-1}) in infiltrated tobacco (A,B) or faba bean (C,D) leaves. A, C: Lesions formed
283 in infiltrated leaf areas. B, D: Quantitative evaluation of CDI activity of WT and mutants' secretomes. Values are
284 the means of at least three experiments and two or three leaves per experiment. One-way ANOVA followed by
285 Dunnett's multiple comparison post hoc test; ***p<0.01; ***p<0.001 (n≥15 for tobacco, n≥8 for faba bean).
286 E: Cell death inducing activity on faba bean leaves of non-proteinaceous (<10kDa) secretome fractions of a 10x
287 mutant and a 12xbb mutant unable to synthesize botrydial and botcinin. F: Effects of heating (95°C for 20 min)
288 on CDI activity of the non-proteinaceous fraction of the 10x mutant. E, F: Student t-test; **p<0.01 (n=6).

11

Discussion

For the generation of multiple mutants with standard mutagenesis techniques, the availability of selection markers is quickly becoming limiting. With a mutated version of *Bcpos5* conferring resistance to the fungicide cyprodinil, we have established a new selection marker which works with similar efficiency as the established markers HygR, FenR and NatR. The advantage of the fungicide resistance markers FenR and CypR is their low cost, because selection can be applied with commercial fungicide formulations. Using the four available selection markers, we have constructed a 4x^R mutant (*spl1 xyn11A nep1 nep2*). Compared to WT and the marker-free mutants generated with CRISPR/Cas, this mutant showed a slight growth retardation. Whether this is due to the constitutive expression of the resistance genes is unclear, but highlights a disadvantage of their use for mutant generation. Based on a recently developed CRISPR/Cas method, we have further improved and simplified the protocol for serial introduction of marker-free gene deletions into *B. cinerea*. A highly favorable result was the high proportion of homokaryotic mutants among the primary transformants. *B. cinerea* protoplasts are generated from germlings containing several nuclei, therefore transformants obtained by standard mutagenesis had to be purified via several rounds of single spore isolations (Noda *et al.* 2007). The reason for the rapid homokaryotization is unclear: We assume that either the RNP complexes are able to edit all nuclei in a protoplast, or that only the nucleus that was edited was able to divide in the transformant. The current protocol allows the generation, verification and purification of multiple *B. cinerea* mutants within three to four weeks. We are not aware of reports in which mutants with a similar number of knockouts have been generated in filamentous fungi until now, besides an eight-fold deletion mutant constructed with a non-CRISPR marker replacement approach in *Aspergillus fumigatus* (Hartmann *et al.* 2011). This and other CRISPR/Cas-based strategies now allow to investigate genes and protein families with redundant functions in most filamentous fungi, except for obligate biotrophs for which any stable transformation remains a great challenge (Martínez-Cruz *et al.* 2017).

We have evaluated the role of 12 CDIPs and two phytoxica metabolites by the construction of single and multiple mutants. In agreement with previous reports, mutants in *nep1*, *nep2*, *xyg1* and *hip1* showed normal virulence (Cuesta Arenas *et al.* 2010; Jeblick *et al.* 2020; Zhu *et al.* 2017), as did *gs1* and *plp1* mutants, which have not been described previously. An unexpected result was the absence of significant virulence defects in mutants lacking Xyn11A, Spl1 or Xyl1. These CDIPs have previously been described as virulence factors, based on the analysis of mutants which were also generated in *B. cinerea* strain B05.10 (Brito *et al.* 2006; Frías *et al.* 2011; Yang *et al.* 2018). The discrepancy of these results with our data is difficult to explain, even more as complementation of the published mutants confirmed their reversion to WT phenotypes. A minor role for virulence of *xyn11A* and *spl1* was indicated by the phenotype of the 4x^R mutant. Of the six polygalacturonases encoded in the *B. cinerea* genome, PG1 and PG2 are most highly expressed on transcriptional and proteomic levels early during infection of different tissues (Blanco-Ulate *et al.* 2014; Have *et al.* 2001; Müller *et al.* 2018), and both enzymes have been reported to be required for full virulence (Have *et al.* 1998; Kars *et al.* 2005). Accordingly, the virulence defects of the 11x mutant devoid of *pg1* and the 12x mutant lacking *pg1* and *pg2* were also significantly stronger than that of the 10x mutant, which confirmed the effects of the loss of one or both PG isoforms. Further

12

333 support came from the analysis of an independently constructed *pg1 pg2* mutant, which
334 showed delayed infection on all tested tissues. Considering the redundancy of genes
335 encoding pectin degrading enzymes in the genome of *B. cinerea* (Amselem *et al.* 2011), it is
336 doubtful whether deletion of the remaining endo-PGs would lead to significant further
337 reduction of virulence. Our work also confirms a previous study about the role of the
338 phytoxic metabolites botrydial and botcinin for infection of *B. cinerea* (Dalmais *et al.*, 2011).
339 Here, the 12xbb mutant unable to synthesize the two toxins were significantly less virulent
340 than its 10x mutant parent, on all host tissues tested except on maize leaves. This was
341 confirmed by further phenotypic analysis of a *bot2 boa6* double mutant generated
342 previously (Leisen *et al.* 2020). Beyond its phytotoxicity, botrydial has been shown to have
343 antibacterial properties (Vignatti *et al.* 2020). Recently, we have discovered a group of *B.*
344 *cinerea* field strains which lack the complete botcinin biosynthesis cluster. These strains are
345 less virulent than other *B. cinerea* strains on tomato leaves but not on other host tissues
346 (Plesken *et al.* 2021). These data confirm that botrydial and botcinin together play a
347 significant role for *B. cinerea* pathogenesis, but their mode of action is unknown, and their
348 individual contributions to the infection process remain unclear.

349 The effects of multiple gene knockouts were variable between host tissues: While smaller
350 effects of multiple gene knockouts on virulence were observed on tomato and maize leaves
351 (lesion sizes >60% of WT), multiple knockouts were considerably less virulent on bean leaves
352 and apple fruit (lesion sizes down to 30% of WT). CDIPs are known to have low plant species
353 specificity, in contrast to many effector proteins from biotrophic and hemibiotrophic fungi.
354 Nevertheless, differences in sensitivity to CDIPs could be due to the presence of different
355 sets of matching receptors or targets in different plant species, or different effects of their
356 activation on plant cell death and defence. PRRs of *B. cinerea* CDIPs belong to the group of
357 receptor like proteins (LRR-RLPs), which have a plant genus- or subgenus-specific distribution
358 (Albert *et al.*, 2020). For example, the receptor of PG1/PG2, RBPG1 has been identified in
359 some but not all accessions of Arabidopsis (Zhang *et al.* 2014). No evidence for similar PG
360 receptors exist in tobacco and broad bean leaves, which respond with necrosis only after
361 treatment with enzymatically active but not inactive PGs (Kars *et al.* 2005). Similarly, Hip1
362 was found to be highly toxic to tobacco but only weakly active in Arabidopsis (Jeblick *et al.*
363 2021). Furthermore, the membrane-directed toxicity of necrosis and ethylene inducing
364 proteins including Nep1 and Nep2 is known to be restricted to dicots (Lenarčič *et al.* 2017).

365 The virulence defects observed for the multiple knockout mutants were less pronounced
366 than expected from the high expression levels of most CDIPs and phytotoxins, and from the
367 virulence phenotypes reported for single knockout mutants in previous studies. Because of
368 the lack of virulence defects in the single mutants and only small incremental differences in
369 virulence between the multiple mutants order, it was difficult to estimate the role of single
370 CDIPs, and it remained unclear if all of them contribute to infection. In case of additive and
371 redundant effects, sequential knockouts would result in a stepwise decrease in virulence.
372 This could uncover virulence effects that are too small to be detected in single mutants, for
373 example in *spl1*, *xyn11A*, *nep1* and *nep2* in the 4x[R] mutant. In case of synergism between
374 CDIPs, a stronger decrease in virulence of a multiple mutant than expected from the
375 contributions of the individual gene knockouts would be observed. Synergism has been

376   shown for botrydial and botcinin, since only the double mutant but not the single mutants
377   revealed significant effects on virulence (Dalmais *et al.* 2011). A third possibility, referred to
378   as 'overkill', assumes that the total CDI activity of the WT exceeds the requirement for
379   pathogenesis under the chosen infection conditions, and predicts that effects on virulence
380   become evident only when the remaining CDI activity falls below a certain threshold. In this
381   case, deletion of few CDIPs would cause no effects, but the decrease in virulence would be
382   stronger when more CDIPs are deleted. Apart from the botrydial/ botcinin synergism, the
383   moderate but significant virulence phenotypes of the multiple mutants argue for
384   predominantly additive effects. An overkill mechanism still seems possible, and could be
385   revealed if further CDIP knockouts would show increasing effects.

386   Microscopic analysis revealed a delay of the 12xbb and 12xpg mutants in the early stages of
387   infection. These data demonstrate a role of one or several of the deleted CDIPs in early stages
388   of host attack, in agreement with observations made with *B. cinerea* strains overexpressing
389   *xyg1* which showed evidence for accelerated infection (Zhu *et al.* 2017). However, the
390   markedly reduced infection of all multiple mutants on apple fruits, which are inoculated via
391   wounds, show that several of the deleted CDIPs are also involved in lesion expansion.

392   The *on planta* secretome of *B. cinerea* is highly phytotoxic, causing cell death in leaf tissue
393   even after five- to ten-fold dilution, down to concentrations of 1 µg ml^{-1}. The secretomes of
394   the 10x and 12x mutants were less toxic compared to WT, but retained substantial
395   phytotoxic activity which could be attributed mostly to the protein fraction. Comparison of
396   the 10x and 12xbb mutant secretomes allowed to assign the remaining, heat-stable
397   phytotoxic activity in the low molecular weight (non-proteinaceous) fraction to botrydial and
398   botcinin. Since this fraction was almost nontoxic in the 12xbb mutant, we conclude that
399   probably no other phytotoxic metabolites are secreted in significant amounts during
400   infection of *B. cinerea*. Therefore, the remaining phytotoxic activity in the 12x mutants is due
401   to further, as yet uncharacterized CDIPs. These include Crh1, a newly described CDIP that
402   has been shown to be translocated via infection cushions into host cells (Bi *et al.* 2021).
403   Several CDIPs have been recently described in two molds related to *B. cinerea*, *Monilinia*
404   *fructigena* (Vilanova *et al.* 2021) and *Sclerotinia sclerotiorum* (Seifbarghi *et al.* 2020), and
405   homologs for them also exist in *B. cinerea*.

406   Taken together, our data demonstrate that the grey mould fungus releases a large number
407   of relatively non host-specific CDIPs and two toxins during infection, which collectively
408   determine its necrogenic ability. We assume that the complexity and redundance of the
409   phytotoxic secretome is correlated with the exceptionally wide host range and the ability of
410   *B. cinerea* to successfully attack more than 1400 reported plant species (Elad Y *et al.* 2016).
411   To gain a deeper insight into the mechanisms of host cell death induction, it is necessary to
412   identify the receptors or targets of the CDIPs in order to study their mode of action.

Materials and Methods

Cultivation and transformation of *Botrytis*

B. cinerea strains were routinely cultured on agar containing malt extract (ME) medium (Müller *et al.* 2018). For growth tests, agar plates containing Gamborg minimal medium (GB5) containing 25 mM glucose were used and ME medium for sporulation tests. For these tests, 10 µl droplets containing 10^5 conidia ml^{-1} were inoculated onto agar plates, and incubated at 20-22°C.

Classical transformation using knockout constructs with resistance markers was performed as described (Leisen *et al.* 2020; Müller *et al.* 2018). Protoplasts transformed with constructs containing CypR cassettes were selected in SH agar containing 0.3 µg ml^{-1} Cyp (Syngenta, Chorus® fungicide formulation). Non-transformed colonies appeared with a frequency of <10^{-7} per transformed protoplast. Resistant colonies were transferred after three days to plates containing GB5 agar with 25 mM glucose and 0.3 µg ml^{-1} Cyp. For generation of marker-free multiple knockout mutants, the transformation protocol of (Leisen *et al.* 2020) was modified as following: To 2x 10^7 *B. cinerea* protoplasts suspended in 100 µl TMSC buffer, 10 µg pTEL-Fen and up to four RNPs, each consisting of pre-complexed 6 µg Cas9-Stu^{2x} and 2 µg sgRNA (two RNPs per gene) were added. The transformed protoplasts were mixed with liquified 200 ml SH agar adjusted to 39.5°C, and poured into ten 90 mm petri dishes. After three days of incubation at 20-22°C, small agarose pieces containing individual transformants were cut out with a scalpel and transferred to 5 cm plates containing selection-free 4x ME agar (4x ME: 4% malt extract, 1.6% glucose, 1.6% yeast extract, 1.5% agar, pH 5.5), to accelerate growth and sporulation of freshly generated transformants. After two days, Plates with no or very little growth were discarded. Hyphal tips of fast growing colonies were transferred to new 4x ME plates and allowed to grow for 5-6 days until sporulation. Conidia or sporulating mycelium were used for DNA isolation and PCR analysis to detect the desired editing events in each of the two genes and the absence of WT DNA in the deleted region. Transformants with deletions of one or both targeted genes were used for phenotypic characterization. Sometimes a single spore isolation was subsequently performed. The resulting culture was used for confirmation of the editing events, and proof of homokaryosis and absence of WT DNA using primers that amplified an internal sequence of the deleted regions.

DNA manipulations

To generate a cyprodinil resistance (CypR) cassette, the *Bcpos5* (Bcin10g02880) coding sequence including two introns was amplified by PCR from genomic DNA of *B. cinerea* B05.10, by using primers CypR_ol_Ptrp_FW CypR_ol_TniaD_RV. The 3'-terminal primer CypR_ol_TniaD_RV was changed in sequence to generate the cypR-associated L412F substitution (Mosbach *et al.* 2017). The resulting fragment was flanked with fragments containing the *Aspergillus nidulans trpC* promoter (PtrpC) generated with primers Gib_pTEL_S_EcorV_PtrpC & PtrpC_ol_CypR_RV, and the *niaD* terminator of *B. cinerea* (TniaD) generated with primers TniaD_ol_CypR_FW & Gib_pTEL_S_EcorV_TniaD, both amplified from plasmid pTEL-Fen (Leisen *et al.* 2020). The CypR cassette was integrated into

15

455   pTEL-Start linearized with EcoRV. To test its functionality as a resistance marker, the CypR
456   cassette was attached to ca. 1 kb flanking regions of several target genes, using a modular
457   cloning approach (see below). After transformation into *B. cinerea* protoplasts, selection was
458   applied in SH agar with 0.3 µg ml^{-1} Cyp. Single spores of the transformants were transferred
459   to Gamborg GB5 minimal medium with 25 mM glucose, supplemented with 0.3 µg ml^{-1} Cyp,
460   for further cultivation and verification of the transformants.

461   Deletion constructs were generated with resistance cassettes for nourseothricin (natR/^{N})
462   and cyprodinil (cypR/^{C}) for *spl1^{C}*, *xyn11A^{N}*, *nep2^{N}*, *ieb1^{C}*, *xyg1^{C}*, *xyn11A^{C}*, and *nep2^{C}*. For this,
463   0.5 - 1 kb genomic regions flanking the coding sequences were amplified, spliced together
464   with a resistance cassette (*trpC* promoter- resistance gene – *niaD* terminator) into a pBS-KS
465   vector by Gibson assembly, and transformed into *E. coli*. Before transformation into *B.*
466   *cinerea*, deletion constructs were released from the plasmids by restriction digestion.

467   For generation of a quadruple mutant, a *xyn11A^{N}* mutant was transformed with a *spl1^{C}* k.o.
468   cassette to generate a *xyn11A^{N} spl1^{C}* double mutant. This mutant was cotransformed with
469   two Cas9-sgRNA complexes targeting *nep1* and *nep2*, and *nep1^{H} nep2^{F}* k.o. cassettes with 60
470   bp homology flanks (amplified using pTEL-Fen or pTEL-Hyg as template) as repair templates.
471   Transformants with resistance to FenR and HygR were tested for the knockout of *nep1* and
472   *nep2*. The double mutant pg1pg2^{R}, kindly provided by Jan van Kan (Wageningen University),
473   was constructed transforming a hygR *pg1* mutant (Have *et al.* 1998) with a *pg2^{N}* knockout
474   construct. The knockouts of *pg1* and *pg2* were confirmed by PCR. The primers used for
475   synthesis of sgRNAs, construction of knockout constructs, and screening of transformants
476   for correct knockouts and homokaryosis are shown in Table S3.

477

478   <u>Infection tests and secretome analyses</u>
479   Infection tests were performed with attached leaves of *Phaseolus vulgaris* (genotype
480   N9059), detached leaves of tomato (*Solanum lycopersicum*, cv. Marmande) and maize (*Zea*
481   *mays*, cv. Golden Bantam), and to apple fruit (Malus domestica, cv. Golden Delicious). Leaf
482   inoculations were performed as previously described (Schamber *et al.* 2010), using 20 µl
483   droplets with 10^{5} conidia ml^{-1} in GB5 minimal medium (GB5: 3.05 g l-1 GB5, 10 mM KH$_2$PO$_4$,
484   pH 5.5) with 25 mM glucose. To achieve maximal accuracy and comparability, two or three
485   droplets each of WT and mutant conidial suspensions were applied on both sides of the
486   midrib of one leaf or leaflet. Apple fruit was inoculated after wounding with a cork borer of
487   7 mm diameter along the equatorial line. Lesions were measured after 48 to 96 h by a caliper
488   or image analysis using ImageJ software, and lesion areas calculated after subtraction of the
489   inoculation area.

490   *On planta* secretomes were obtained from detached tomato leaves densely inoculated with
491   25 µl droplets containing 10^{5} conidia ml^{-1}, and incubated at 20-22°C and 100% humidity in
492   flat glass trays covered with saran wrap. After 48 h, droplets were collected, frozen at -80°C,
493   thawed, centrifuged at 4°C for 60 min at 4000 g, sterile filtered and again frozen in aliquots
494   at -80°C until further analysis. MS/MS-based proteomic analysis for confirmation of loss of
495   CDIPs in the deletion mutants was performed as described (Müller *et al.* 2018). To determine
496   CDI activity of WT and mutant secretomes, the secretomes (containing ca. 5-10 µg protein

497   ml^{-1}) were diluted with GB5 medium to concentrations of 1 or 2 µg protein ml^{-1}, and ca. 20-
498   50 µl each of the solutions were infiltrated into *Nicotiana benthamiana* or *Vicia faba* (cv.
499   Fuego) leaves. The size of necrotic lesions in the infiltrated leaf area was recorded after two
500   days. Heat treatments of the secretome were performed by incubation for 20 min at 95°C in
501   a heating block. Size fractionation of the secretomes was done using ultrafiltration cartridges
502   (Amicon Ultra-4, Merck Millipore Ltd, Tullagreen, Co., Cork, Ireland) with 10 kDa molecular
503   weight cutoff. Before infiltration into leaves, the low molecular weight fraction was two-fold
504   concentrated.

Microscopic analysis of infection

507   To compare the early infection process of *B. cinerea* WT and multi-k.o. mutants
508   microscopically, inoculations of detached *Phaseolus vulgaris* leaves and onion epidermal
509   layers were performed. From onions, epidermal layers were removed from the concave side,
510   fixed with tape onto glass coverslips and killed by incubation at 65°C for 30 min in a water
511   bath. After thorough washing with water, samples were dried and inoculated with 20 µl
512   droplets $5*10^4$ conidia ml^{-1} in 1 mM fructose, and incubated in a humid chamber for 24 h.
513   For confocal microscopy, *Phaseolus vulgaris* leaves were inoculated with 1 µl of 10^5 conidia
514   ml^{-1} in GB5 medium with 25 mM glucose. After 24 h, developing lesions were stained with
515   10µg ml^{-1} calcofluor white (fluorescence brightener 28, Sigma) for 5 min and thoroughly
516   washed subsequently. Images were acquired using a Zeiss LSM880 AxioObserver confocal
517   laser scanning microscope equipped with a Zeiss EC Plan-Neofluar 5x/0.16 M27 objective
518   (DFG, INST 248/254-1). Fluorescent signals of calcofluor white (excitation/emission 405
519   nm/410-523-571 nm) and chlorophyll (excitation/emission 633nm/638-721 nm) were
520   processed using the Zeiss software ZEN 2.3 or ImageJ (https://imagej.nih.gov/ij/).

Statistical analyses

523   Statistical analyses were carried out with the GraphPad Prism software. For comparison of
524   radial growth, means of three experiments, with three replicates each, were analysed by one
525   way ANOVA followed by Dunnett's multiple comparisons post-hoc test. For infection assays,
526   two or three pairwise inoculations of WT and mutant were performed on the same leaf or
527   fruit (Fig. 2). Relative necrotic areas (% of WT) were calculated for each leaf/fruit, based on
528   technical replicates of WT vs. mutant pairs. Values from at least three inoculation dates with
529   at least three leaves/fruits each were analyzed by one-sample t test. Comparison of relative
530   necrotic areas between different deletion mutants was carried out by one-way ANOVA
531   followed by Tukey's multiple comparison test. Box limits of box plots represent 25th
532   percentile and 75th percentile, horizontal line represents median, and whiskers display
533   minimum to maximum values. Evaluation of MS/MS proteomics data for significant
534   deviations in the abundance of detected proteins in WT and 10x, 11x, 12xbb and 12xpg
535   mutants was performed using the Perseus bioinformatics platform (Tyanova *et al.* 2016).

546 **References**

547 Albert, I. Böhm, H. Albert, M. Feiler, C.E. Imkampe, J. Wallmeroth, N. Brancato, C. Raaymakers, T.M.
548   Oome, S. Zhang, H. Krol, E. Grefen, C. Gust, A.A. Chai, J. Hedrich, R. van den Ackerveken, G. and
549   Nürnberger, T. (2015) An RLP23-SOBIR1-BAK1 complex mediates NLP-triggered immunity. *Nature*
550   *Plants,* 1, 15140. DOI: 10.1038/nplants.2015.140

551 Amselem, J. Cuomo, C.A. van Kan, J.A.L. Viaud, M. Benito, E.P. Couloux, et al., (2011) Genomic analysis
552   of the necrotrophic fungal pathogens *Sclerotinia sclerotiorum* and *Botrytis cinerea*. *PLoS Genetics,*
553   7, e1002230. DOI: 10.1371/journal.pgen.1002230

554 Bi, K. Scalschi, L. Jaiswal, N. Mengiste, T. Fried, R. Sanz, A.B. Arroyo, J. Zhu, W. Masrati, G., Sharon, A.
555   (2021) The *Botrytis cinerea* Crh1 transglycosylase is a cytoplasmic effector triggering plant cell death
556   and defense response. *Nature Communications,* 12, 2166. DOI: 10.1038/s41467-021-22436-1

557 Blanco-Ulate, B. Morales-Cruz, A. Amrine, K.C.H. Labavitch, J.M. Powell, A.L.T. and Cantu, D. (2014)
558   Genome-wide transcriptional profiling of *Botrytis cinerea* genes targeting plant cell walls during
559   infections of different hosts. *Frontiers in Plant Science,* 5, 435. DOI: 10.3389/fpls.2014.00435

560 Brito, N. Espino, J.J. and González, C. (2006) The endo-beta-1,4-xylanase xyn11A is required for
561   virulence in *Botrytis cinerea*. *Molecular Plant-Microbe Interactions,* 19, 25–32. DOI: 10.1094/MPMI-
562   19-0025

563 Choquer, M. Rascle, C. Gonçalves, I.R. Vallée, A. de, Ribot, C. Loisel, E. Smilevski, P. Ferria, J. Savadogo,
564   M. Souibgui, E. Gagey, M.-J. Dupuy, J.-W. Rollins, J.A. Marcato, R. Noûs, C. Bruel, C. and Poussereau,
565   N. (2021) The infection cushion of *Botrytis cinerea*: a fungal 'weapon' of plant-biomass destruction.
566   *Environmental Microbiology,* 23, 2293–2314. DOI: 10.1111/1462-2920.15416

567 Cuesta Arenas, Y. Kalkman, E.R. Schouten, A. Dieho, M. Vredenbregt, P. Uwumukiza, B. Ruiz, M.O. and
568   van Kan, J.A. (2010) Functional analysis and mode of action of phytotoxic Nep1-like proteins of
569   *Botrytis cinerea*. *Physiological and Molecular Plant Pathology,* 376–386. DOI:
570   10.1016/j.fgb.2017.02.001

571 Dalmais, B. Schumacher, J. Moraga, J. Le Pêcheur, P. Tudzynski, B. Collado, I.G. and Viaud, M. (2011)
572   The *Botrytis cinerea* phytotoxin botcinic acid requires two polyketide synthases for production and
573   has a redundant role in virulence with botrydial. *Molecular Plant Pathology,* 12, 564–579. DOI:
574   10.1111/j.1364-3703.2010.00692.x

575 Doehlemann, G. Berndt, P. and Hahn, M. (2006) Different signalling pathways involving a Galpha
576   protein, cAMP and a MAP kinase control germination of *Botrytis cinerea* conidia. *Molecular*
577   *Microbiology,* 59, 821–835. DOI: 10.1111/j.1365-2958.2005.04991.x

578 Elad Y, Pertot I, Prado AMC and Stewart A (2016) Plant hosts of *Botrytis* spp. *In: Elad Y; Vivier M;*
579   *Fillinger S (ed), Botrytis, the good, the bad*, 413–486.

18

580   Franco-Orozco, B. Berepiki, A. Ruiz, O. Gamble, L. Griffe, L.L. Wang, S. Birch, P.R.J. Kanyuka, K. and
581   Avrova, A. (2017) A new proteinaceous pathogen-associated molecular pattern (PAMP) identified
582   in Ascomycete fungi induces cell death in Solanaceae. *The New Phytologist,* 214, 1657–1672. DOI:
583   10.1111/nph.14542

584   Frías, M. Brito, N. and González, C. (2013) The Botrytis cinerea cerato-platanin BcSpl1 is a potent
585   inducer of systemic acquired resistance (SAR) in tobacco and generates a wave of salicylic acid
586   expanding from the site of application. *Molecular Plant Pathology,* 14, 191–196. DOI:
587   10.1111/j.1364-3703.2012.00842.x

588   Frías, M. González, C. and Brito, N. (2011) BcSpl1, a cerato-platanin family protein, contributes to
589   *Botrytis cinerea* virulence and elicits the hypersensitive response in the host. *The New Phytologist,*
590   192, 483–495. DOI: 10.1111/j.1469-8137.2011.03802.x

591   Frías, M. González, M. González, C. and Brito, N. (2016) BcIEB1, a *Botrytis cinerea* secreted protein,
592   elicits a defense response in plants. *Plant Science* 250, 115–124. DOI:
593   10.1016/j.plantsci.2016.06.009

594   Frías, M. González, M. González, C. and Brito, N. (2019) A 25-Residue Peptide From *Botrytis cinerea*
595   Xylanase BcXyn11A Elicits Plant Defenses. *Frontiers in Plant Science,* 10. DOI:
596   10.3389/fpls.2019.00474

597   Govrin, E.M. and Levine, A. (2000) The hypersensitive response facilitates plant infection by the
598   necrotrophic pathogen *Botrytis cinerea*. *Current biology : CB,* 10, 751–757. DOI: 10.1016/s0960-
599   9822(00)00560-1

600   Hahn, M. and Scalliet, G. (2021) One Cut to Change Them All: CRISPR/Cas, a Groundbreaking Tool for
601   Genome Editing in *Botrytis cinerea* and Other Fungal Plant Pathogens. *Phytopathology,* 111, 474–
602   477. DOI: 10.1094/PHYTO-09-20-0379-PER

603   Hartmann, T. Cairns, T.C. Olbermann, P. Morschhäuser, J. Bignell, E.M. and Krappmann, S. (2011)
604   Oligopeptide transport and regulation of extracellular proteolysis are required for growth of
605   *Aspergillus fumigatus* on complex substrates but not for virulence. *Molecular Microbiology*, 82,
606   917–935. DOI: 10.1111/j.1365-2958.2011.07868.x

607   Have, A. ten, Mulder, W. Visser, J. and van Kan, J.A. (1998) The endopolygalacturonase gene Bcpg1 is
608   required for full virulence of *Botrytis cinerea*. *Molecular Plant-Microbe Interactions,* 11, 1009–1016.
609   DOI: 10.1094/MPMI.1998.11.10.1009

610   Have, A. ten, Breuil, W.O. Wubben, J.P. Visser, J. and van Kan, J.A. (2001) *Botrytis cinerea*
611   endopolygalacturonase genes are differentially expressed in various plant tissues. *Fungal Genetics*
612   *and Biology : FG & B,* 33, 97–105. DOI: 10.1006/fgbi.2001.1269

613   Heye, U.J. Speich, J. Siegle, H. Steinemann, A. Forster, B. Knauf-Beiter, G. Herzog, J. and Hubele, A.
614   (1994) CGA 219417: a novel broad-spectrum fungicide. *Crop Protection*, 13, 541–549.

615   Jeblick, T. Leisen, T. Steidele, C.E. Müller, J. Mahler, F. Sommer, F. Keller, S. Hückelhoven, R. Hahn, M.
616   and Scheuring, D. (2020) The secreted hypersensitive response inducing protein 1 from *Botrytis*
617   *cinerea* displays non-canonical PAMP-activity. BioRxiv preprint doi:
618   https://doi.org/10.1101/2020.12.16.423131

619   Kars, I. Krooshof, G.H. Wagemakers, L. Joosten, R. Benen, J.A.E. and van Kan, J.A.L. (2005) Necrotizing
620   activity of five *Botrytis cinerea* endopolygalacturonases produced in *Pichia pastoris*. *The Plant*
621   *Journal* 43, 213–225. DOI: 10.1111/j.1365-313X.2005.02436.x

622   Leisen, T. Bietz, F. Werner, J. Wegner, A. Schaffrath, U. Scheuring, D. Willmund, F. Mosbach, A. Scalliet,
623   G. and Hahn, M. (2020) CRISPR/Cas with ribonucleoprotein complexes and transiently selected
624   telomere vectors allows highly efficient marker-free and multiple genome editing in *Botrytis*
625   *cinerea*. *PLoS Pathogens,* 16, e1008326. DOI: 10.1371/journal.ppat.1008326

626   Lenarčič, T. Albert, I. Böhm, H. Hodnik, V. Pirc, K. Zavec, A.B. Podobnik, M. Pahovnik, D. Žagar, E. Pruitt,
627   R. Greimel, P. Yamaji-Hasegawa, A. Kobayashi, T. Zienkiewicz, A. Gömann, J. Mortimer, J.C. Fang, L.

628 Mamode-Cassim, A. Deleu, M. Lins, L. Oecking, C. Feussner, I. Mongrand, S. Anderluh, G. and
629 Nürnberger, T. (2017) Eudicot plant-specific sphingolipids determine host selectivity of microbial
630 NLP cytolysins. *Science (New York, N.Y.),* 358, 1431–1434. DOI: 10.1126/science.aan6874

631 Li, H. Zhang, Z. Qin, G. He, C. Li, B. and Tian, S. (2020) Actin Is Required for Cellular Development and
632 Virulence of *Botrytis cinerea* via the Mediation of Secretory Proteins. *mSystems,* 5. DOI:
633 10.3389/fgene.2020.00661

634 Martínez-Cruz, J. Romero, D. Vicente, A. de and Pérez-García, A. (2017) Transformation of the cucurbit
635 powdery mildew pathogen *Podosphaera xanthii* by *Agrobacterium tumefaciens*. *The New
636 Phytologist,* 213, 1961–1973. DOI: 10.1111/nph.14297

637 Mosbach, A. Edel, D. Farmer, A.D. Widdison, S. Barchietto, T. Dietrich, R.A. Corran, A. and Scalliet, G.
638 (2017) Anilinopyrimidine Resistance in *Botrytis cinerea* Is Linked to Mitochondrial Function.
639 *Frontiers in Microbiology,* 8, 2361. DOI: 10.3389/fmicb.2017.02361

640 Müller, N. Leroch, M. Schumacher, J. Zimmer, D. Könnel, A. Klug, K. Leisen, T. Scheuring, D. Sommer,
641 F. Mühlhaus, T. Schroda, M. and Hahn, M. (2018) Investigations on VELVET regulatory mutants
642 confirm the role of host tissue acidification and secretion of proteins in the pathogenesis of *Botrytis
643 cinerea*. *The New Phytologist,* 219, 1062–1074. DOI: 10.1111/nph.15221

644 Nafisi, M. Stranne, M. Zhang, L. van Kan, J.A.L. and Sakuragi, Y. (2014) The endo-arabinanase BcAra1 is
645 a novel host-specific virulence factor of the necrotic fungal phytopathogen *Botrytis cinerea*.
646 *Molecular plant-microbe interactions,* 27, 781–792. DOI: 10.1094/MPMI-02-14-0036-R

647 Nie, J. Yin, Z. Li, Z. Wu, Y. and Huang, L. (2019) A small cysteine-rich protein from two kingdoms of
648 microbes is recognized as a novel pathogen-associated molecular pattern. *The New Phytologist,*
649 222, 995–1011. DOI: 10.1111/nph.15631

650 Nie, J. Zhou, W. Liu, J. Tan, N. Zhou, J.-M. and Huang, L. (2021) A receptor-like protein from *Nicotiana
651 benthamiana* mediates VmE02 PAMP-triggered immunity. *The New Phytologist,* 229, 2260–2272.
652 DOI: 10.1111/nph.16995

653 Noda, J. Brito, N. Espino, J.J. and González, C. (2007) Methodological improvements in the expression
654 of foreign genes and in gene replacement in the phytopathogenic fungus *Botrytis cinerea*.
655 *Molecular Plant Pathology,* 8, 811–816. DOI: 10.1111/j.1364-3703.2007.00432.x

656 Noda, J. Brito, N. and González, C. (2010) The *Botrytis cinerea* xylanase Xyn11A contributes to virulence
657 with its necrotizing activity, not with its catalytic activity. *BMC Plant Biology,* 10, 38. DOI:
658 10.1186/1471-2229-10-38

659 Ono, E. Mise, K. and Takano, Y. (2020) RLP23 is required for Arabidopsis immunity against the grey
660 mould pathogen *Botrytis cinerea*. *Scientific Reports,* 10, 13798. DOI: 10.1038/s41598-020-70485-1

661 Pinedo, C. Wang, C.-M. Pradier, J.-M. Dalmais, B. Choquer, M. Le Pêcheur, P. Morgant, G. Collado, I.G.
662 Cane, D.E. and Viaud, M. (2008) Sesquiterpene synthase from the botrydial biosynthetic gene
663 cluster of the phytopathogen *Botrytis cinerea*. *ACS Chemical Biology,* 3, 791–801. DOI:
664 10.1021/cb800225v

665 Plesken, C. Pattar, P. Reiss, B. Noor, Z.N. Zhang, L. Klug, K. Huettel, B. and Hahn, M. (2021) Genetic
666 Diversity of Botrytis cinerea Revealed by Multilocus Sequencing, and Identification of *B. cinerea*
667 Populations Showing Genetic Isolation and Distinct Host Adaptation. *Frontiers in Plant Science*
668 12:663027. DOI: 10.3389/fpls.2021.663027

669 Ron, M. and Avni, A. (2004) The Receptor for the Fungal Elicitor Ethylene-Inducing Xylanase Is a
670 Member of a Resistance-Like Gene Family in Tomato. *The Plant Cell,* 16, 1604–1615. DOI:
671 10.1105/tpc.022475

672 Schamber, A. Leroch, M. Diwo, J. Mendgen, K. and Hahn, M. (2010) The role of mitogen-activated
673 protein (MAP) kinase signalling components and the Ste12 transcription factor in germination and
674 pathogenicity of *Botrytis cinerea*. *Molecular Plant Pathology*, 11, 105-119. DOI: 10.1111/j.1364-
675 3703.2009.00579.x

676 Seidl, M.F. and van den Ackerveken, G. (2019) Activity and Phylogenetics of the Broadly Occurring
677 Family of Microbial Nep1-Like Proteins. *Annual Review of Phytopathology*. 57:367-386. doi:
678 10.1146/annurev-phyto-082718-100054

679 Seifbarghi, S. Borhan, M.H. Wei, Y. Ma, L. Coutu, C. Bekkaoui, D. and Hegedus, D.D. (2020) Receptor-
680 Like Kinases BAK1 and SOBIR1 Are Required for Necrotizing Activity of a Novel Group of *Sclerotinia*
681 *sclerotiorum* Necrosis-Inducing Effectors. *Frontiers in Plant Science,* 11:1021. DOI:
682 10.3389/fpls.2020.01021

683 Stefanato, F.L. Abou-Mansour, E. Buchala, A. Kretschmer, M. Mosbach, A. Hahn, M. Bochet, C.G.
684 Métraux, J.-P. and Schoonbeek, H. (2009) The ABC transporter BcatrB from *Botrytis cinerea* exports
685 camalexin and is a virulence factor on Arabidopsis thaliana. *The Plant Journal,* 58, 499–510. DOI:
686 10.1111/j.1365-313X.2009.03794.x

687 Thomma, B.P.H.J. Nürnberger, T. and Joosten, M.H.A.J. (2011) Of PAMPs and effectors: the blurred PTI-
688 ETI dichotomy. *The Plant Cell,* 23, 4–15. DOI: 10.1105/tpc.110.082602

689 Tyanova, S. Temu, T. Sinitcyn, P. Carlson, A. Hein, M.Y. Geiger, T. Mann, M. and Cox, J. (2016) The
690 Perseus computational platform for comprehensive analysis of (prote)omics data. *Nature Methods,*
691 13, 731–740. DOI: 10.1038/nmeth.3901

692 Veloso, J. and van Kan, J.A.L. (2018) Many Shades of Grey in *Botrytis*-Host Plant Interactions. *Trends in*
693 *Plant Science,* 23, 613–622. DOI: 10.1016/j.tplants.2018.03.016

694 Vignatti, P. Gonzalez, M.E. Jofré, E.C. Bolívar-Anillo, H.J. Moraga, J. Viaud, M. Collado, I.G. and
695 Pieckenstain, F.L. (2020) Botrydial confers *Botrytis cinerea* the ability to antagonize soil and
696 phyllospheric bacteria. *Fungal Biology,* 124, 54–64. DOI: 10.1016/j.funbio.2019.11.003.

697 Vilanova, L. Valero-Jimenez, C.A. and van Kan, J.A. (2021) Deciphering the *Monilinia fructicola* genome
698 to discover effector genes possibly involved in virulence. *Genes,* 12, 568. DOI:
699 10.3390/genes12040568

700 Weiberg, A. Wang, M. Lin, F.-M. Zhao, H. Zhang, Z. Kaloshian, I. Huang, H.-D. and Jin, H. (2013) Fungal
701 small RNAs suppress plant immunity by hijacking host RNA interference pathways. *Science (New*
702 *York, N.Y.),* 342, 118–123. DOI: 10.1126/science.1239705

703 Yang, Y. Yang, X. Dong, Y. and Qiu, D. (2018) The *Botrytis cinerea* Xylanase BcXyl1 Modulates Plant
704 Immunity. *Frontiers in Microbiology,* 9, 2535. DOI: 10.3389/fmicb.2018.02535

705 You, Y. and van Kan, J.A.L. (2021) Bitter and sweet make tomato hard to (b)eat. *The New Phytologist,*
706 230, 90–100. DOI: 10.1111/nph.17104

707 Zhang, L. Kars, I. Essenstam, B. Liebrand, T.W.H. Wagemakers, L. Elberse, J. Tagkalaki, P. Tjoitang, D.
708 van den Ackerveken, G. and van Kan, J.A.L. (2014) Fungal endopolygalacturonases are recognized
709 as microbe-associated molecular patterns by the Arabidopsis receptor-like protein
710 RESPONSIVENESS TO BOTRYTIS POLYGALACTURONASES1. *Plant Physiology,* 164, 352–364. DOI:
711 10.1104/pp.113.230698

712 Zhang, W. Fraiture, M. Kolb, D. Löffelhardt, B. Desaki, Y. Boutrot, F.F.G. Tör, M. Zipfel, C. Gust, A.A. and
713 Brunner, F. (2013) Arabidopsis receptor-like protein30 and receptor-like kinase suppressor of BIR1-
714 1/EVERSHED mediate innate immunity to necrotrophic fungi. *The Plant Cell,* 25, 4227–4241. DOI:

715 Zhang, Y. Zhang, Y. Qiu, D. Zeng, H. Guo, L. and Yang, X. (2015) BcGs1, a glycoprotein from *Botrytis*
716 *cinerea*, elicits defence response and improves disease resistance in host plants. *Biochemical and*
717 *Biophysical Research Communications,* 457, 627–634. DOI: 10.1016/j.bbrc.2015.01.038

718 Zhu, W. Ronen, M. Gur, Y. Minz-Dub, A. Masrati, G. Ben-Tal, N. Savidor, A. Sharon, I. Eizner, E. Valerius,
719 O. Braus, G.H. Bowler, K. Bar-Peled, M. and Sharon, A. (2017) BcXYG1, a Secreted Xyloglucanase
720 from *Botrytis cinerea*, Triggers Both Cell Death and Plant Immune Responses. *Plant Physiology,* 175,
721 438–456. DOI: 10.1104/pp.17.00375

722

723

Supplemental Figures and Tables
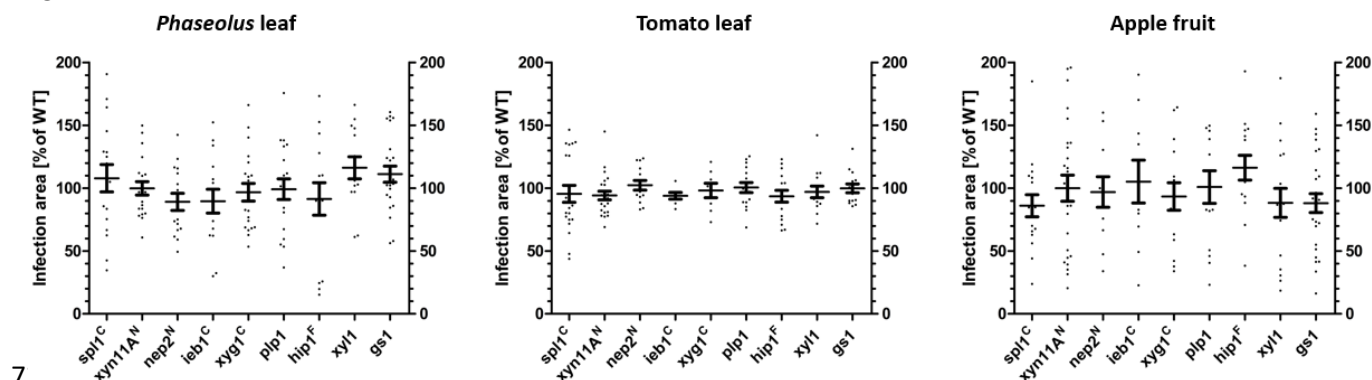
Figure S1: Infection tests with single CDIP mutants. The p values by one-sample t test to a hypothetical value of 100% (WT) did not show significant diferences for any of the tested mutants.
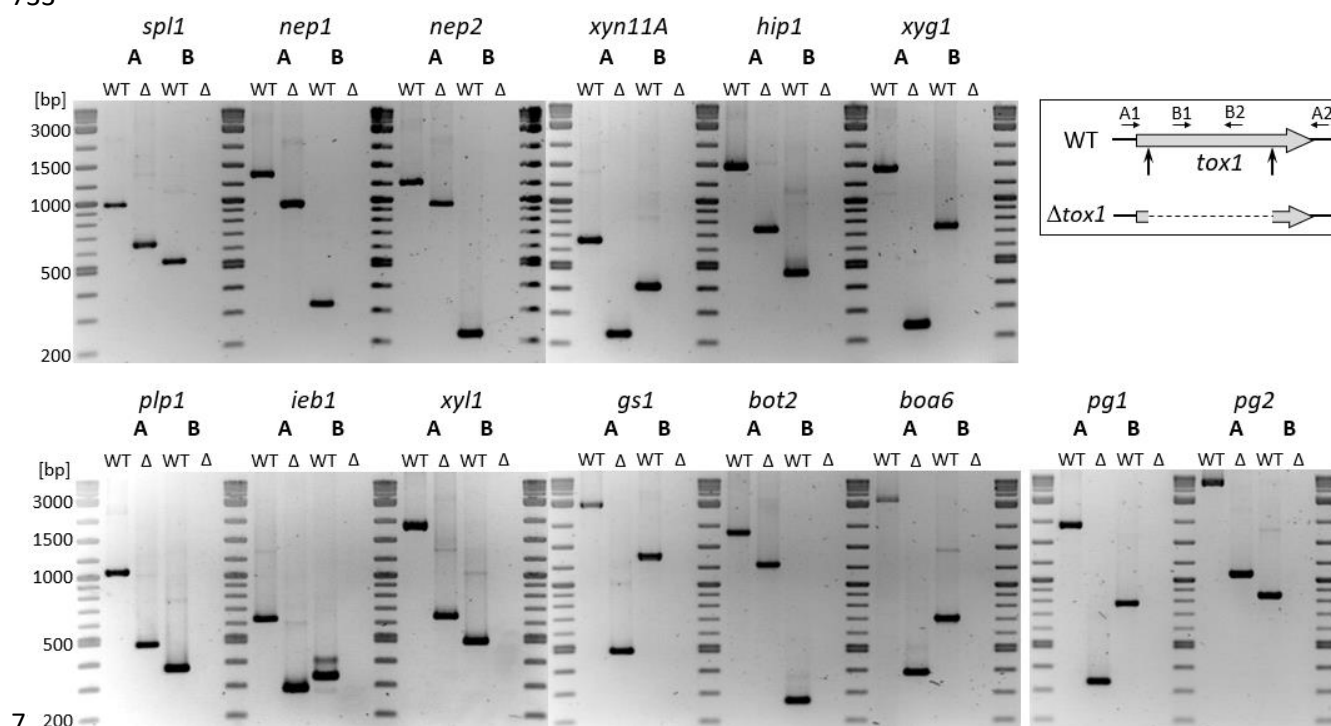

Figure S2: PCR-based confirmation of gene deletions in the 12xbb mutant. Position of primer pairs used are indicated in the sketch. A: PCR with primers flanking the deleted region B: PCR with primers amplifying an internal part of the deleted region. Missing PCR products in reactions B confirm homokaryosis of deletion mutants. The size of the deletions was determined by sequencing (Table S2). Primers used are shown in Table S4. Mapping of *pg1* and *pg2* deletions was done with the 12xpg mutant.
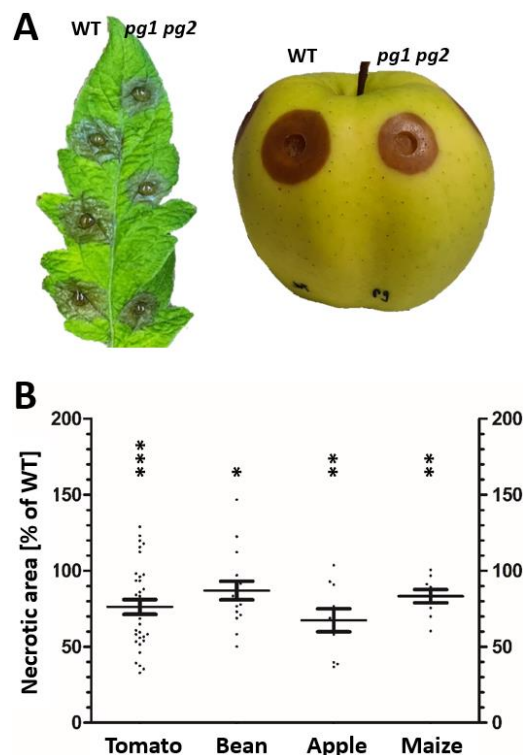
Figure S3: Characterization of a *pg1 pg2* double mutant (provided by J. van Kan). A:: Infected tomato leaf (72 h) and apple fruit (96 h). B: Results of infection tests on different plant tissues (cf. Fig. 1). The p values by one-sample t test to a hypothetical value of 100% (WT) are indicated. * p value < 0.05; ** p value < 0.01; *** p value < 0.001.
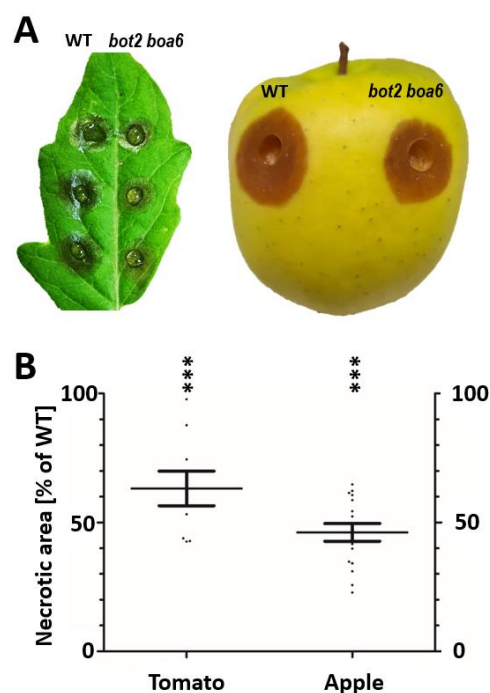
Figure S4: Lesion formation of the *B. cinerea bot2 boa6* mutant (Leisen *et al*. 2020) on tomato leaf (48 h) and apple fruit (96 h), compared to WT. The p values by one-sample t test to a hypothetical value of 100% (WT) are indicated *** p value < 0.001.
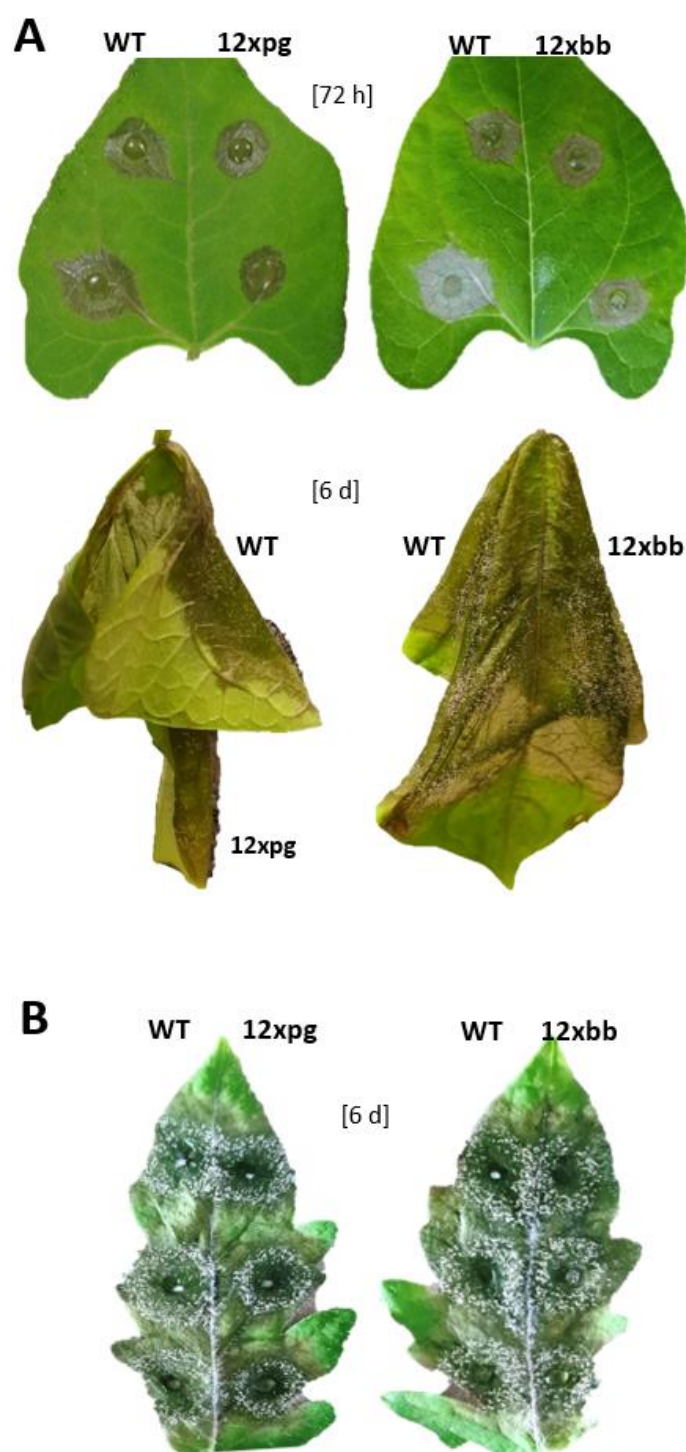
23

753

Figure S5: Lesion formation and sporulation of *B. cinerea* WT, 12xpg and 12xbb mutants on attached *Phaseolus* bean leaves (A: 3 days; B: 6 days), and on detached tomato leaves (6 days).

756

24

757   Table S1: Mapping of the deletions in the 12xbb and 12xpg (*pg1* and *pg2* only) mutants.

Gene	Accession	Protein size (aa)	Deletion mapping			
			Predicted	Obtained	Size (change)	Deleted codons
spl1	Bcin03g00500	137	3:185840-186170	as expected	331 bp	24-end*
nep1	Bcin06g06720	246	6:2351724-2352121	as expected	398 bp	34-end*
nep2	Bcin02g07770	244	2:2793732-2794002	as expected	271 bp	80-133
xyn11A	Bcin03g00480	227	3:174482-174915	as expected	434 bp	64-end*
hip1	Bcin14g01200	151	14:538686-539428	14:538687-539428	742 bp (-1)	all
xyg1	Bcin03g03630	248	3:1224165-1225358	3:1224166-1225358	1193 bp (-1)	all
plp1	Bcin10g01020	147	10:417795-418359	10:417796-418359	564 bp (-1)	all
ieb1	Bcin15g00100	187	15:78364-78704	as expected	341 bp	20-115
xyl1	Bcin09g01800	329	9:672899-674137	as expected	1239 bp	all
gs1	Bcin04g04190	645	4:1491835-1494178	as expected	2344 bp	all
bot2	Bcin12g06390	399	12:2224281-2224868	as expected	588 bp	157-end*
boa6	Bcin01g00060	2460	1:18020-20645	as expected	2626 bp	661-end*
pg1	Bcin14g00850	382	14:371069-372695	14:371071-372695	1625 bp (-2)	all
pg2	Bcin14g00610	374	14:247707 to 249005	14:245745 to 250019	1299 / 4275**	all

758   Deletions were predicted based on the expected cleavage sites of each pair of Cas9-RNP. * Deletion of codons
759   due to frameshift. **The 4275 bp (instead of 1299 bp) deletion extended into Bcin14g00600 encoding a sclerotia-
760   specifically expressed polyketide synthetase. Since this gene is not expressed *in planta*, it is not expected to
761   contribute to infection.

25

762   **Table S2**: MS/MS-detection of CDIPs in the secretomes of *B. cinerea* WT and multiple k.o. mutants.

	n		Spl1*	Nep2	Xyn11A	Hip1	XYG1	IEB1	Gs1	PG1*	PG2*
WT	6	mean	560.332	41.818	337.044	48.416	595.662	509.355	406.258	697.042	1.184.440
		st.dev.	409.251	21.637	377.637	81.950	393.979	351.129	282.887	856.712	1..157307
4x^R	5	mean	0	0	0	8.355	609.594	564.152	475.172	937.821	1.213.902
		st.dev.	0	0	0	16.710	489.109	553.043	299.148	1.306.651	1.017.928
pg1 pg2	4	mean	377.472	25.224	273.638	13.480	931.655	415.655	436.435	274	250
		st.dev.	420.371	16.477	226.923	23.348	825.703	190.870	306.249	474	432

	n										
WT	5	mean	4.292.542	712.180	9.987.220	269.486	2.946.020	4.583.840	3.756.580	7.239.160	5.246.700
		st.dev.	2.427.053	177.747	1.684.412	330.555	935.540	1.328.030	498.726	1.554.149	2.604.637
10x	4	mean	1.771	0	0	0	0	0	0	880.6725	2.772.025
		st.dev.	3.067	0	0	0	0	0	0	2.207.591	58.036
11x	3	mean	32.047	0	0	0	0	0	0	16.757	12.606.067
		st.dev.	24.337	0	0	0	0	0	0	23.698	2.980.671
12xpg	3	mean	3.545	0	0	0	0	0	0	27.588	19.550
		st.dev.	5.013	0	0	0	0	0	0	12.016	27.648
12xbb	3	mean	46.996	0	0	0	0	0	0	7.956.433	9.498.333
		st.dev.	23.050	0	0	0	0	0	0	1.672.172	6.315.201

763   Mean LQF intensities are shown. Proteomic analysis was performed in two series of experiments, the
764   first series including WT, 4x^R and *pg1 pg2* mutants, and the second series WT, 10x, 11x, 12xpg and
765   12xbb mutants. n: Number of replicates. Values of proteins that have been deleted in the analysed
766   mutants are shown with red background. *The low intensity values observed for Spl1, PG1 and PG2
767   are probably due to carry-over of some peptides from WT samples during MS/MS analysis.
768

769

770

771   **Table S3**: Oligonucleotides used.

Primer Name	Sequence	use
Gib_pTEL_S_EcorV_PtrpC	AGCTGATGATCACTTAAGAACGCGTAGATCATTTTTTGGGC TTGGCTGG	Amplification of P*trpC*
PtrpC_ol_CypR_RV	CCCTCGGAAACATTTGGATGCTTGGGTAGAATAGGT	
CypR_ol_Ptrp_FW	CCCAAGCATCCAAATGTTTCCGAGGGTGTTGCC	Amplification of CypR
CypR_ol_TniaD_RV	CTCTCAGTTACTTATTCTTCGCCAAAAGGATGGTTGAACTT CAGGAACC	
TniaD_ol_CypR_FW	ACCATCCTTTTGGCGAAGAATAAGTAACTGAGAGGTGGTTT AGATATGG	Amplification of T*niaD*
Gib_pTEL_S_EcorV_TniaD	CAATTCCTAGGTCTAGATGCATGCAGATCTCACTGATACAT CTGGCACC	
xyn11A_KO-Fl_l_FW	CCCCCTCGAGGTCGACGGTATCGATAAGCTTGATCCCTCAC ATCAAGTGTATGTGAT	Amplification of left flank for *xyn11A* knockout
xyn11A_KO-Fl_l_RW	CATGCATGTGAGCAAAAGGCCAGCAAAGTTGATTGTAGTAG AGTATGTAGATGAGAT	
xyn11A_KO-Fl_r_FW	CATTTGCGGGTCCTTTCCGGCGATCGACGGTTCCACATACA AGATCC	Amplification of right flank for *xyn11A* knockout
xyn11A_KO-Fl_r_RW	AGAACTAGTGGATCCCCCGGGCTGCAGGAATTCGATAGAAA TGGGTGATGAGTATGTAGGTTATT	
R-Casette_FW	TGCTGGCCTTTTGCTCACATGCATG	Amplification of resistance cassettes from pTEL vectors
R-Casette_RV	ATCGCCGGAAAGGACCCGCAAATG	
xyg1_KO_left_FW	CCCCCTCGAGGTCGACGGTATCGATAAGCTTGATGAATTGC CAAAGTACAGCTTCAAACTTCTA	Amplification of left flank for *xyg1* knockout
xyg1_KO-left_RW	CATGCATGTGAGCAAAAGGCCAGCAGAATGTTTGAATGAAG GAAAAGAAGAGCG	
xyg1_KO-right_FW	CATTTGCGGGTCCTTTCCGGCGATGATGCGAATCTATCTAA AGAGTGATATTGT	Amplification of right flank for *xyg1* knockout
xyg1_KO-right_RW	AGAACTAGTGGATCCCCCGGGCTGCAGGAATTCGATAATTT ACGCGAGGGGAAGCTT	
ieb1_KO-left_FW	CCCCCTCGAGGTCGACGGTATCGATAAGCTTGATCCTTGTA CCCTTTGTGCATAGCTAG	Amplification of left flank for *ieb1* knockout

ieb1_KO-left_RW	CATGCATGTGAGCAAAAGGCCAGCATTGTGTATTTGGTTGCTTGATATGAAGAT	
ieb1_KO-right_FW	CATTTGCGGGTCCTTTCCGGCGATTGATTAGTTCCTTGGCGACATTGC	Amplification of right flank for *ieb1* knockout
ieb1_KO-right_RW	AGAACTAGTGGATCCCCCGGGCTGCAGGAATTCGATGGTGACATGAGCCTTGATTCTATGTATATTC	
spl1_KO-left_FW	CCCCCTCGAGGTCGACGGTATCGATAAGCTTGATAATTCTCGTGTTGTTGTCGAACAAAC	Amplification of left flank for *spl1* knockout
spl1_KO-left_RW	CATGCATGTGAGCAAAAGGCCAGCAACATCATGTCTTATATACCTTCTACCCCTC	
spl1_KO-right_FW	CATTTGCGGGTCCTTTCCGGCGATATAGGAAGTGGAAGAATGGGATAGG	Amplification of right flank for *spl1* knockout
spl1_KO-right_RW	AGAACTAGTGGATCCCCCGGGCTGCAGGAATTCGATGCTGAGGTGTAAGGAAATGGTGGA	
nep2_KO-left_FW	CCCCCTCGAGGTCGACGGTATCGATAAGCTTGATCCGAATCACGAAAGAAAGTTTTGTAG	Amplification of left flank for *nep2* knockout
nep2_KO-left_RW	CATGCATGTGAGCAAAAGGCCAGCAACTACATTCTACAAGAGGAAACGCA	
nep2_KO-right_FW	CATTTGCGGGTCCTTTCCGGCGATGGCTATATTCTGGGAGTCTATTGGC	Amplification of right flank for *nep2* knockout
nep2_KO-right_RW	AGAACTAGTGGATCCCCCGGGCTGCAGGAATTCGATATGTGAGAGGTTAATCGACATTTAGAATGAG	
nep1 KO F	CAGCATCAACAGCATCAGCTTCCATTCCATATTCATTACATTCCACATTACCACTTTCGTATCGCCGGAAAGGACCCGCAAATG	Amplification of *nep1*-hygR repair template
nep1 KO R	ACGATCTCTGACAGGACAAACTTCCAGATTCTCCAGAACTCTATCTAGTAAGAAAGAACTTGCTGGCCTTTTGCTCACATGCATG	
nep2 KO F	CACACATCTATTAATCGCTCTCTCCTCTTAGTTACAAGGAAAATCCAGACAAACTTCATCTGCTGGCCTTTTGCTCACATGCATG	Amplification of nep2-fenR repair template
nep2 KO R	GCAAAAGCCAATAGACTCCCAGAATATAGCCCCTTATATTCATACATAAAGACACAAAGTATCGCCGGAAAGGACCCGCAAATG	
nep1 gRNA 1	AAGCTAATACGACTCACTATAGCGCTTGGGTCAACAACCCCGGTTTTAGAGCTAGAAATAGCAAG	sgRNA synthesis for *nep1*
nep2 gRNA 1	AAGCTAATACGACTCACTATAGTATGTTCGAGGAGGACAAAGGTTTTAGAGCTAGAAATAGCAAG	sgRNA synthesis for *nep2*
gRNA _reverse	AAAAGCACCGACTCGGTGCCACTTTTTCAAGTTGATAACGGACTAGCCTTATTTTAACTTGCTATTTCTAGCTCTAAAAC	Constant oligonucleotide for sgRNA synthesis
Uni KO fw	CATTTGCGGGTCCTTTCCGGCGAT	universal oligo for 3′-integration
Uni KO rev	CATGCATGTGAGCAAAAGGCCAGCA	universal oligo for 5′-integration
xyn11A_5′for	CCCTTTTGTGAAACAACCTGGA	Proof of integration 5′-flank *xyn11A*
xyn11A_3′rev	GGAGATGTGACGGTGAGGATAT	Proof of integration 3′-flank xyn11A
nep2_5′for	CATCTACCAGCCCACTCAGAT	Proof of integration 5′-flank *nep2N*
nep2_3′rev	CTTCTCCTTTCATTCATGCATATCGC	Proof of integration 3′-flank *nep2N*
pTrpC_rev	ACCGCCTGGACGACTAAAC	Proof of integration 5′-flank *ieb1*
ieb1_5′for	GTCTCACAGTTGTCGCTGG	Proof of integration 5′-flank *ieb1*
ieb1_3′rev	GACCGTCGAAAACGCAAAG	Proof of integration 3′-flank *ieb1*
spl1_5′for	ATTAACTTCGACGTCGTCGAC	Proof of Integration 5′-flank *spl1*
spl1_3′rev	GTGGATGGAATTCTTGAACTCAGTC	Proof of integration 3′-flank S*spl1*
xyg_5for	GTCAAGGTTGTACGACTTTATCCAT	Proof of Integration 5′-flank *xyg1*
xyg_3rev	GTTCGAAGGGTTTGTCGATGA	Proof of integration 3′-flank *xyg1*
WT_Screen_fw	GAGAATCACGACAATGCAAGA	Proof of Integration 5′-flank *nep1H*
TL144 Nep1 seq R	CGTTGGCTTATTCAATGCGGAGG	Proof of integration 3′-flank *nep1H*
TL145 Nep2 seq F	GAACTTTGAATAGTGGGCAGTTGGG	Proof of Integration 5′-flank *nep2F*
TL146 Nep2 seq R	ACAAGGCGACCATGATTATTTCTGG	Proof of integration 3′-flank *nep2F*
Bcxyn11A_KO_Confirm_F	TGAATGTCTTGCAAGAAAGAG	*xyn11AN* WT check
Bcxyn11A_KO_Confirm_R	ATTTAAGAAACAGTGATGGAAGC	
Bcxyg_KO_Confirm_FW	GTTTCCTTAGTCTTGGCAACA	*xyg1C* WT check
Bcxyg_KO_Confirm_RW	GGTTGGCAGTCAAGTATGTAA	
Bcspl1_q_F	CCACCCAAGGTTCCCTCAAG	*spl1C* WT check
Bcspll_KO_Confirm_RW	CTCCAACCATTTACAATCCACA	
Bcnep2_KO-Confirm_FW	ATGGTTGCCTTCTCAAAATC	*nep2N* WT check
Bcnep2_KO-Confirm_RW	GGTTGTTTTCCACCAACAGTA	

Bcieb1_KO_Confirm_FW	ATGTTCTCCAAGACCTTCATC	ieb1[C] WT check
Bcieb1_KO_Confirm_RW	CCATTCTTGATTTAAGCGTACT	
Bcnep1_KO-Confirm_FW	CATTTCTCCAACGCAAAATTC	nep1[H] WT check
Bcnep1_KO-Confirm_RW	GGAAGGAGACATAGTATTCGAC	
Bcnep2_KO-Confirm_FW	ATGGTTGCCTTCTCAAAATC	nep2[F] WT check
Bcnep2_KO-Confirm_RW	GGTTGTTTTCCACCAACAGTA	
pg1_ndel_FW	CAACATATGACCGCAGCTCCAAACCC	pg1 KO Check
pg1_EcoRI_RV	GTTGAATTCTTAACACTTGACACCAGATGGGAGACC	
trpC-Screen	AGGAATCCGCTCTTGGCTCCAC	Proof of integration 3'-flank pg1
natR-F	CTTCGTGGTCGTCTCGTACT	Proof of integration 3'-flank pg2
PG_RTR	CCAGCACAAGCCTTCTTAAC	
TL246 spl1-gRNA 1	AAGCTAATACGACTCACTATAGATCATCGTAGCCAACGTCGTGTTTTAGAGCTAGAAATAGCAAG	Synthesis of spl1 sgRNAs
TL247 spl1-gRNA 2	AAGCTAATACGACTCACTATAGCAAGTCGACAAGAGTGCTTGGTTTTAGAGCTAGAAATAGCAAG	
TL252_spl1_F	TGACAATGCACACAATGCGG	spl1 KO check
TL253_spl1_R	TCCGAACATTCCGAGCTTCC	
spl1_del-seq	CAAAATGCAATTCCCAACTC	spl1 KO sequencing
spl1_wt_F	CCACCCAAGGTTCCCTCAAG	spl1 WT check
spl1_wt_R	TCCGAACATTCCGAGCTTCC	
TL238_Bcnep1_gRNA_3	AAGCTAATACGACTCACTATAGATGGAGTCATGAGGAACGAGTTTTAGAGCTAGAAATAGCAAG	Synthesis of nep1 sgRNAs
TL 167_Bcnep1_gRNA 2	AAGCTAATACGACTCACTATAGACCTCCGACGACGTTTCCAGGTTTTAGAGCTAGAAATAGCAAG	
TL143 Nep1 seq F	TCTGGTGCCGATTGAATACATCAAGTG	nep1 KO check
TL144 Nep1 seq R	CGTTGGCTTATTCAATGCGGAGG	
Bcnep1_KO-Confirm_FW	CATTTCTCCAACGCAAAATCC	nep1 KO sequencing
TL267_Nep1_WT_F	CATGACTCCATCAACCCATGGG	nep1 WT check
TL268_Nep1_WT_R	GAAAGGGATACTTACACCAGGCG	
TL 169 Bcnep2 gRNA 2	AAGCTAATACGACTCACTATAGTTACACCTTCCCAATCGTGAGTTTTAGAGCTAGAAATAGCAAG	Synthesis of nep2 sgRNAs
TL241_Bcnep2_gRNA_4	AAGCTAATACGACTCACTATAGTCGATGCATCGGGTAACACAGTTTTAGAGCTAGAAATAGCAAG	
TL145 Nep2 seq F	GAACTTTGAATAGTGGGCAGTTGGG	nep2 KO check
TL146 Nep2 seq R	ACAAGGCGACCATGATTATTTCTGG	
Nep2_RT_fw	CAGTGGGACCGTAGGAACAG	nep2 KO sequencing
TL269_Nep2_WT_F	CTCTTCCACACGATTGCTATTGAGTC	nep2 WT check
Nep2_RT_rev	GGCTCGTCCTTTGGCATGTAC	
TL243_BcXyn11a_gRNA_2	AAGCTAATACGACTCACTATAGGTGGTGTTACATACTCCAAGTTTTAGAGCTAGAAATAGCAAG	Synthesis of xyn11A sgRNAs
TL245_BcXyn11a_gRNA_4	AAGCTAATACGACTCACTATAGAAAATGGTTTGCAGTGGTGAGTTTTAGAGCTAGAAATAGCAAG	
Bcxyn11A_KO_Confirm_FW	TGAATGTCTTGCAAGAAAGAG	xyn11A KO check
Bcxyn11A_KO_Confirm_RW	ATTTAAGAAACAGTGATGGAAGC	
Bcxyn11A_KO-Confirm_FW	TGAATGTCTTGCAAGAAAGAG	xyn11A KO sequencing
TL285_WT_Xyn_F	GGTCAATATGCCGTAAGCTGGAC	xyn11A WT check
BcXylA.rv	CGTACGCTTGCTAGTACGGAC	
TL288_Hip1_gRNA5	AAGCTAATACGACTCACTATAGACAATGCCGATCTGTGGAGAGTTTTAGAGCTAGAAATAGCAAG	Synthesis of hip1 sgRNAs
TL 163 HIP gRNA 3 GFP	AAGCTAATACGACTCACTATAGCTTGGACTACAGCTCCTAGGTTTTAGAGCTAGAAATAGCAAG	
KO_Hip1_3'flank_seq	TGGCTAGTTTCTGGAGCTGTTG	hip1 KO check
KO_Hip1_5'flank_seq	GTGATACATACTTGTCATGGGATG	
KO_Hrp1_5'flank_seq	GTGATACATACTTGTCATGGGATG	hip1 KO sequencing
Bcin14g01200_FW_Ndel	CAACATATGGCCATCGAGAAGCGCAGCAG	hip1 WT check
Bcin14g01200_RV_EcoRI	TGTGAATTCCTAGGAGCTGTAGTCCAAGCCGAA	
TL291_Xyg1_gRNA5	AAGCTAATACGACTCACTATAGTTAAGGAACTGAGATGTGCGGTTTTAGAGCTAGAAATAGCAAG	Synthesis of xyg1 sgRNAs
TL290_Xyg1_gRNA4	AAGCTAATACGACTCACTATAGACTTTCTAAAATGCTCAACAGTTTTAGAGCTAGAAATAGCAAG	
TL292_Xyg_F	TGAGCGCTCGTAACATGATATCCG	xyg1 KO check
TL293_Xyg_R	TGAAATCTGGCCAACGTTCAAATCC	
TL292_Xyg_F	TGAGCGCTCGTAACATGATATCCG	xyg1 KO sequencing
Bcxyg_KO_Confirm_FW	GTTTCCTTAGTCTTGGCAACA	xyg1 WT check
Bcxyg_KO_Confirm_RW	GGTTGGCAGTCAAGTATGTAA	
TL310 sgRNA_RLP30_lig_1	AAGCTAATACGACTCACTATAGATGGGAGAGATGATTTGAGGTTTTAGAGCTAGAAATAGCAAG	Synthesis of plp1 sgRNAs
TL313 sgRNA_RLP30_lig_4	AAGCTAATACGACTCACTATAGAGTGAGGTAGTGGTTGAAAGGTTTTAGAGCTAGAAATAGCAAG	
TL306_RLP30_lig-F	ATCTTTCCATCGTCCCATAATCCC	plp1 KO check
TL307_RLP30_lig-R	GGGTTTGGAGAACTCGTGATCG	
TL307_RLP30_lig-R	GGGTTTGGAGAACTCGTGATCG	plp1 KO sequencing
TL308_RLP30_lig_WT-F	CAGCACTCTTGCAACCGCTAC	plp1 WT check
TL309_RLP30_lig_WT-R	GTTGTTCCAACTCCCGTGCTG	
TL_259_ieb1_gRNA4	AAGCTAATACGACTCACTATAGAGCACGTGCAGAGACAATGGGTTTTAGAGCTAGAAATAGCAAG	Synthesis of ieb1 sgRNAs
TL176_Bcieb1_gRNA_1	AAGCTAATACGACTCACTATAGCACTCCGCCGATACCCACGGGTTTTAGAGCTAGAAATAGCAAG	
Bcieb1_KO_Confirm_FW	ATGTTCTCCAAGACCTTCATC	ieb1 KO check
Bcieb1_KO_Confirm_RW	CCATTCTTGATTTAAGCGTACT	

Bcieb1_KO-Confirm_RW	CCATTCTTGATTTAAGCGTACT	*ieb1* KO sequencing
TL286_WT_Ieb_F	CTGCACGTGCTGCAAGC	*ieb1* WT check
TL287_WT_Ieb_R	GGGTATCGGCGGAGTGTGG	
TL319_sgRNA_Xyl_2	AAGCTAATACGACTCACTATAGTTACCAAACATAAAGAC AGGTTTTAGAGCTAGAAATAGCAAG	Synthesis of *xyl1* sgRNAs
TL320_sgRNA_Xyl_3	AAGCTAATACGACTCACTATAGGCATAAAAGTAATTATC CGGTTTTAGAGCTAGAAATAGCAAG	
TL322_Xyl1_KO_sc_F	ATTTACGTCGGTCACAGCGG	*xyl1* KO check
TL323_Xyl1_KO_sc_R	ACTCTACTCTGCAAACCCGC	
TL345_Xyl_F	CTGCATCTAGGCTGCGCAAT	*xyl1* KO sequencing
TL324_Xyl1_WT_F	CTCGAGTGTTTGGTCCCTCC	*xyl1* WT check
TL325_Xyl1_WT_R	GACGCAACGATATCGGGGAT	
TL_327_Gs1_gRNA6	AAGCTAATACGACTCACTATAGTCAAGACACCTAGTATC CAAGTTTTAGAGCTAGAAATAGCAAG	Synthesis of *gs1* sgRNAs
TL_328_Gs1_gRNA7	AAGCTAATACGACTCACTATAGAGTGGTAGCTGGTAATC GTGGTTTTAGAGCTAGAAATAGCAAG	
TL_330_Gs1_F	GAGGAAGGGGAGGAAAATCAAGG	*gs1* KO check
TL_331_Gs1_R	ACACATGATGTCAGGCTTTGATG	
TL330	GAGGAAGGGGAGGAAAATCAAGG	*gs1* KO sequencing
TL 93 Gs1 Ct FW	ATGCAATATCGGCGCAGATGG	*gs1* WT check
TL 94 Gs1 CT RV	GTTGCGACGACATTGACGTAGC	
TL_256_Bot2_gRNA3	AAGCTAATACGACTCACTATAGCTGCTTCACCTCCTCCG CTGGTTTTAGAGCTAGAAATAGCAAG	Synthesis of *bot2* sgRNAs
TL_266_Bot2_gRNA5	AAGCTAATACGACTCACTATAGACAAAACATCATTCACC CTGGTTTTAGAGCTAGAAATAGCAAG	
TL 91 Bot2 CT FW	GTCATCTCGGCGTCCTGTATG	*bot2* KO check
Bot2_RT_rev	CCCTCAGGACCCAAGTAAC	
TL 133 Bot2 KO F	CGACGATCGTACGTTGCTCTTAGTCATTGGACG	*bot2* KO sequencing
TL 92 Bot2 CT RV	AAGAACTGGAGCAGTGTTGTC	*bot2* WT check
Bot2_B0510_rev	GTGGATAGACCAGCACAAAC	
TL_263_Boa6_gRNA4	AAGCTAATACGACTCACTATAGACGATAGTAAGCGATAC GAAGTTTTAGAGCTAGAAATAGCAAG	Synthesis of *boa6* sgRNAs
TL_265_Boa6_gRNA6	AAGCTAATACGACTCACTATAGAACCAGGTAAACCAGCC ATGGTTTTAGAGCTAGAAATAGCAAG	
TL347_Boa6_F	TGCACAATGGCCGGCAATG	*boa6* KO check
TL348_Boa6_R	GAGATAGTGGGACGATATGGTCGC	
TL 128 Boa6 KO F	CACTTCGTGAGCTTCCAGATGCTCCGAAATGG	*boa6* KO sequencing
TL 90 Boa6 CT RV	CATTGTCTCCACGAGATAGCACTC	*boa6* WT check
TL157 Boa6 WT FW	GGGGTCACATTCTCTGCTGTAGTCGG	
TL294_Pg1_gRNA1	AAGCTAATACGACTCACTATAGTTGATGCGAAATGTTAA CAGGTTTTAGAGCTAGAAATAGCAAG	Synthesis of *pg1* sgRNAs
TL296_Pg1_gRNA3	AAGCTAATACGACTCACTATAGAAGAGAAGACTGATAAC AGGTTTTAGAGCTAGAAATAGCAAG	
TL298_Pg1_F	GCCCATTCAACAAGAAAGTGGTG	*pg1* KO check
TL299_Pg1_R	CCGCTATATTGGCGAATGACAACC	
TL298_Pg1_F	GCCCATTCAACAAGAAAGTGGTG	*pg1* KO sequencing
Bcpg1_KO_Confirm_F	ATGGTTCAACTTCTCTCAATG	*pg1* WT check
Bcpg1_KO_Confirm_R	GATATCGGAGACAGTGTTGTC	
TL300_Pg2_gRNA1	AAGCTAATACGACTCACTATAGTGGAGCTGCAGACACCA AAGGTTTTAGAGCTAGAAATAGCAAG	Synthesis of *pg2* sgRNAs
TL302_Pg2_gRNA3	AAGCTAATACGACTCACTATAGACAATGGTTGATAACCA TGGTTTTAGAGCTAGAAATAGCAAG	
TL305_Pg2_R	CCACCCAATATCTAACCACCAAATGC	*pg2* KO check
TL358_Pg2_L_F	TCCGTATGGTCAGCTCCAGACC	
TL356_Pg2_R_R	ATGACACAGGGTCGTGGGAT	
TL353_Pg2_L_F	TCCATTCCGGCTTCCACTTCG	
TL353 _Pg2_L_F	TCCATTCCGGCTTCCACTTCG	*pg2* KO sequencing
Bcpg2_KO_Confirm_FW	ATGGTTCATATCACAAGCCTT	*pg2* WT check
Bcpg2_KO_Confirm_RW	TCCACCGGTGAAAGTAATG	

772